Unveiling *Wolbachia pipientis* transcriptomic signature in *Aedes aegypti*: a comprehensive meta-analysis

Sebastián Mejías[1], Natalia E. Jiménez[1,2,3*], Carlos Conca[1,4], J. Cristian Salgado[1], Ziomara P. Gerdtzen[1]

[1]Centre for Biotechnology and Bioengineering (CeBiB), Department of Chemical Engineering, Biotechnology and Materials, University of Chile, Santiago, Chile

[2]Instituto de Ingeniería Biológica y Médica, Escuelas de Ingeniería, Medicina y Ciencias Biológicas, Pontificia Universidad Católica de Chile, Santiago, Chile

[3]Departamento de Ingeniería Química y Bioprocesos, Facultad de Ingeniería, Pontificia Universidad Católica de Chile, Santiago, Chile

[4]Center for Mathematical Modeling (CMM) (UMI CNRS 2807), Department of Mathematical Engineering, University of Chile, Santiago, Chile

*Corresponding author

E-mail: natalia.jimenez@uc.cl

Abstract

The mosquito *Aedes aegypti*, main vector of arboviruses such as Dengue and Zika, causes major health burdens worldwide and is expanding its geographical range. A promising arboviral control strategy consists in replacing native *A. aegypti* populations with others artificially infected with the intracellular bacteria *Wolbachia pipientis*, which reduces the mosquito's vectorial capacity. Despite the current success of this strategy, preserving its efficacy over time will depend on a solid mechanistic knowledge of the *A. aegypti*-*Wolbachia* symbiosis. Previous genome-wide transcriptomic studies have made progress in such understanding but no work has focused on systematically identifying effects of *Wolbachia* that are consistent across datasets. To identify *A. aegypti* genes and functions consistently affected by *Wolbachia*, we performed *de novo* differential expression and gene set enrichment analysis on published *Wolbachia*-infected *A. aegypti* transcriptomic datasets, followed by a meta-analysis of the obtained *p*-values using the maxP method. Individual *de novo* analysis revealed the downregulation of six opsins due to *w*MelPop infection in mosquito heads, which may contribute to the fitness loss that currently impairs the use of this strain for arboviral control. Meta-analysis revealed 31 consistently differentially expressed genes, some of which have escaped the focus of *A. aegypti*-*Wolbachia* research, such as a flavin-containing monooxygenase and farnesoic acid methyltransferases. We also found consistent upregulation of GO terms related to electron transport chain, carbohydrate transmembrane transport and serine-type peptidase activity/inhibition, as well as downregulation of DNA replication. These results motivate new hypotheses on the dominant *A. aegypti* factors involved in *Wolbachia*'s pathogen blocking, such as induction of oxidative stress depending on upregulation of host electron transport chain rather than dual- and NADPH-oxidases, which showed downregulation or no regulation across datasets. This work shows how added value can be obtained from previous experimental efforts, developing integrated insights on biological systems that are not reachable at the time of the original publications.

Author summary

Aedes aegypti is the primary vector for arthropod-borne viruses, including Dengue, Zika, and Chikungunya, which impose severe global health burdens. The geographical range of *Aedes aegypti* is expanding, further exacerbating these challenges. A promising strategy to combat these arboviruses involves artificially infecting native *A. aegypti* mosquitoes with the bacteria *Wolbachia pipientis*, which reduces their competence as vectors. Gene expression studies comparing *Wolbachia*-infected versus uninfected *A. aegypti* have developed mechanistic understanding on this biological system, which is crucial for enhancing *Wolbachia*-based vector control. However, the generality of the observed effects is unclear, as no study has systematically compared the available gene expression profiles from different studies. Here we jointly analyzed gene expression profiles from *Wolbachia*-infected *A. aegypti* in order to identify consistent effects of the bacteria in this host. Our results provided new gene targets and hypotheses relevant for *Wolbachia*-based arboviral control. For example, we found consistent upregulation of *A. aegypti*'s electron transport chain and hypothesized it to be a persistent mechanism of viral blocking, which is essential for the success of the control strategy. Our work illustrates how accumulation of related genome-wide omic datasets and evolution of bioinformatic resources can be leveraged to develop integrated insights into biological systems, maximizing the value of previous experimental efforts.

Introduction

Arboviruses (arthropod-borne viruses) such as Dengue, Zika and Chikungunya (DENV, ZIKV and CHIKV, respectively) impose serious morbidity and mortality burdens worldwide [1–8]. The primary arboviral vector, the mosquito *Aedes aegypti*, has expanded its geographic range and is now prevalent in Africa, Europe, Asia, Oceania and the Americas [3,5,9,10]. This, coupled with a general lack of effective broad-spectrum vaccines and the limitations of insecticide-based vector control, has driven the development of new strategies against arboviral diseases [2,7,11–13].

A recent control method centers around *Wolbachia pipientis*, an obligate intracellular bacteria naturally occurring in nearly half of all insect species [2,14]. *Wolbachia* transfection into *A. aegypti* reduces vectorial

capacity for arboviruses (pathogen blocking, PB), and induces embryo lethality when infected males mate with uninfected females (cytoplasmic incompatibility, CI), conferring a reproductive advantage to infected females [15–17]. These phenotypes have motivated controlled releases of transfected mosquitoes to replace wild *A. aegypti* populations, successfully reducing dengue disease in Indonesia [18], Australia [19] and Brazil [20].

Despite current success, there are critical challenges regarding this strategy, such as optimizing the introduction and spread of *Wolbachia* under adverse selective pressures [21] and avoiding loss of desired phenotypes over time [12]. Solution of these problems will depend on the mechanistic understanding of the *A. aegypti-Wolbachia* symbiosis [17,22,23].

Genome-wide transcriptomic data allows a comprehensive characterization of the molecular players of symbiosis, as well as the biological processes implicated [24]. Consequently, comparative microarray and RNA-Seq analyses of *Wolbachia*-infected versus uninfected *A. aegypti* have made notable progress in determining the impacts of this bacteria on immune response, metabolism, redox homeostasis and behavior, identifying specific mediating host genes [25–31].

Despite these key contributions, the extent to which the effects of *Wolbachia* are shared across datasets is still unclear. While finding consistent effects of *Wolbachia* across *A. aegypti* conditions has been addressed in the context of specific multifactorial experiments [27,31], no study has been dedicated to conciliate all available transcriptomic data accumulated over the last two decades. Uncertainty in this regard may hinder the identification of fundamental symbiotic interactions in this system.

A mere intersection of published results would be unsatisfactory to fill this gap given that: (i) due to the specificity of research questions or limitations of databases at a given time, valuable information often remains concealed within datasets. For instance, despite producing genome-wide transcriptomic data, some authors have focused their functional characterizations on differentially methylated genes [28], long non-coding RNAs [29], immune genes [25] and upregulated genes [27]. (ii) Published results such as sets of differentially expressed genes (DEGs) are often filtered according to significance or effect size, so that mild but consistent effects may

be lost by simply intersecting them. (iii) Technical variability associated with different analysis pipelines may further interfere with identification of consistent effects between studies.

In this work, we present a *de novo* analysis of previously published transcriptomic datasets of *Wolbachia*-infected/uninfected *A. aegypti* using up-to-date bioinformatics databases, and a meta-analysis of the resulting *p*-values to unveil a transcriptomic signature of *Wolbachia* in *A. aegypti*. By addressing limitations in previous analyses and synthesizing results, we aim to contribute significantly to the broader understanding of the *A. aegypti*-*Wolbachia* symbiosis and relevant phenotypes for arboviral control.

Methods

Data acquisition

Comparative genome-wide microarray and RNA-Seq datasets comprising *Wolbachia*-infected and uninfected *A. aegypti* conditions were retrieved from Gene Expression Omnibus [32], Sequence Read Archive [33] and ArrayExpress [34]. Lack of *Wolbachia*-uninfected controls or experimental replication was considered as exclusion criteria (a summary of included and excluded datasets is provided in **S1 Table**).

Microarray data analysis

All analyses were performed using R v4.2.3 [35] with the limma v3.54.2 package [36], with default parameters and standard methods unless stated otherwise. To prevent unreliable microarray spots from affecting normalization steps, weights of outlier and quality flagged spots were set to zero. After background correction, two-channel intensity data was combined into log-ratio values, followed by within- and between-array normalization. Control spots were removed and normalized log-ratios from duplicated spots were averaged before differential expression analysis, contrasting each *Wolbachia*-infected condition to its equivalent uninfected condition. Principal component analysis (PCA) and heatmaps were based on normalized log-intensities for each channel.

To identify functional classes overrepresented among up- or downregulated genes from each dataset, each gene list was sorted in decreasing order according to its logarithmic fold-change and subjected to Gene Set Enrichment Analysis (GSEA) [37] against Gene Ontology functional terms (database version 2024-01) [38]. GSEA was preferred over other methods as it does not require applying arbitrary significance or size-effect cutoffs on differential expression results, which may hinder the identification of functional effects reflected by moderate but coordinated expression changes of several genes [37]. GSEA overcomes this limitation by considering the complete results of a differential expression analysis, quantifying the extent to which the genes from each functional set are enriched towards the up- or downregulated genes via a Normalized Enrichment Score (positive/negative scores reflect up/downregulation, respectively) and its *p*-value [37]. We find this approach particularly valuable as *Wolbachia* is restricted to some host tissues and its effects are to a great extent tissue-specific [30,39], so that local transcriptomic signals may be diluted in whole body RNA samples. *P*-values were Benjamini-Hochberg adjusted to control the False Discovery Rate [51], applying a threshold of 0.05.

RNA-Seq data analysis

Quality of raw *Aedes aegypti* reads was assessed with FastQC v0.11.9 [41]. Trimmomatic v0.38 [42] was used to trim adapter and low quality sequences, using a sliding window approach. STAR v2.7.8a [43] was used to align trimmed reads to the AaegL5 reference genome, with splicing event information obtained from NCBI RefSeq *Aedes aegypti* Annotation Release 101 [44,45]. Aligned reads were counted at gene level using featureCounts v2.0.1 [46] and differential expression analyses were performed using DESeq2 v1.34.0 [47] in R, contrasting each *Wolbachia*-infected condition to its equivalent uninfected condition. GSEA was performed as described previously. Principal component analysis and heatmaps were based on gene counts normalized via the Variance Stabilizing Transformation (VST) from DESeq2 [47].

Meta-analysis

To search for *A. aegypti* genes and functions consistently affected by *Wolbachia* infection, we used the maxP method [48] implemented in the metap R package [49], to combine *p*-values derived from individual

differential expression and GSEA tests. maxP is appropriate for finding non-zero effects in all statistical tests, using the maximum *p*-value as the test statistic [50,51]. Combined *p*-values were adjusted with the Benjamini-Hochberg method to control the False Discovery Rate [51], applying a cutoff of 0.05 for genes and 0.01 for GO terms. Functional gene annotations were retrieved from VectorBase [52], InterPro [53] and Gene Ontology [38].

Results

Overview of datasets

Datasets from five studies published between 2009 and 2023 were selected [25,27,30,31,54], comprising *Wolbachia* strains *w*Mel and *w*MelPop and five kinds of host tissue: whole body, head, muscle, carcass and midgut. All samples were female adults, ranging from 2 to 15 days post-eclosion (**Table 1**).

Table 1. Summary of selected transcriptomic studies.

Study	Accession no. [a]	Assay	Background condition	Experimental groups [b]	Comparison
Kambris et al. (2009) [25]	PRJNA118709	Array	2 and 15 days-old female whole bodies from laboratory lines	A. Line PGYP1 B. Line PGYP1.tet	A vs B
Rancès et al. (2012) [27]	E-MEXP-2931	Array	8 days-old female whole bodies from laboratory lines	A. Line PGYP1 B. Line PGYP1.tet C. Line MGYP2 D. Line MGYP2.tet	A vs B C vs D
Ye et al. (2013) [28]	E-MEXP-2907	Array	15 days-old female tissues from laboratory lines	A. Line PGYP1, head B. Line PGYP1.tet, head C. Line PGYP1, muscle D. Line PGYP1.tet, muscle	A vs B C vs D
Wimalasiri-Yapa et al. (2023) [31]	PRJNA867516	RNASeq	4 days-old female whole bodies from natural populations with given *w*Mel release histories	A. *w*Mel released in 2011 B. *w*Mel released in 2013/14 C. *w*Mel released in 2017 D. No release	A vs D B vs D C vs D

Boehm et al. (2023) [30]	PRJNA949154	RNASeq	7 to 13 days-old female tissues from laboratory lines, at given days post blood feeding (dpf)	A. Line COL.wMel, carcass, 4 dpf B. Line COL.tet, carcass, 4 dpf C. Line COL.wMel, carcass, 7 dpf D. Line COL.tet, carcass, 7 dpf E. Line COL.wMel, midgut, 4 dpf F. Line COL.tet, midgut, 4 dpf G. Line COL.wMel, midgut, 7 dpf H. Line COL.tet, midgut, 7 dpf	A vs B C vs D E vs F G vs H

[a] E-MEXP prefix corresponds to ArrayExpress accession numbers, while PRJNA prefix corresponds to SRA and GEO accession numbers.

[b] Lines PGYP1 and PGYP1.tet: *w*MelPop-transinfected *A. aegypti* and its tetracycline cleared counterpart [25,27,28]. Lines MGYP2 and MGYP2.tet: *w*Mel-transinfected *A. aegypti* and its tetracycline cleared counterpart [27]. Lines COL.wMel and COL.tet: *w*Mel-transinfected Colombian *A. aegypti* and its tetracycline cleared counterpart [30].

All datasets were analyzed *de novo*, yielding reliable results according to intermediate step quality assessments. In particular, >90% reads mapped to the *A. aegypti* reference genome in each RNA-Seq sample (**S2 Table**) and two-channel microarray MA-plots show consistency between expected and observed average intensities and red/green intensity fold-changes for control spots (**S1 Fig**). In the following we present our findings from these new analyses, contrasting them to their original analyses.

Kambris et al. (2009)

Kambris et al. (2009) sought to examine the mechanisms behind the life-shortening phenotype induced by *Wolbachia* in *A. aegypti*, comparing whole-body transcriptome of female *w*MelPop-infected *A. aegypti* (line PGYP1) versus tetracycline-treated PGYP1 cells to remove *Wolbachia* infection (line PGYP1.tet). Four two-channel Agilent microarray slides were competitively hybridized to PGYP1 and PGYP1.tet cDNA samples, each sample derived from an independent pool of 2- and 15-days-old mosquitoes. Microarray analysis was conducted with Genespring GX software and differentially expressed genes (DEGs) were obtained by subjecting normalized logarithmic intensity ratios to *t*-tests against zero, with a *p*-value threshold of 0.05. No functional enrichment analysis of DEGs was performed [25]. Our own analysis yielded new insights into the transcriptomic effect of *w*MelPop on *A. aegypti* (**Fig 1**).

Fig 1. Transcriptomic effects of *w*MelPop on female *A. aegypti* whole bodies assessed from the analysis of the dataset in Kambris et al. (2009). (A) PCA of normalized log-intensities. (B) Hierarchical biclustering of z-scores from normalized log-intensities. Column names denote slides and channels, with R for red and G for green. (C) Top 20 GSEA results obtained from this dataset.

Infection status was not the main source of variation in this dataset **(Figs 1.A and 1.B)**. Indeed, PCA showed that the first principal component correlates with slides rather than infection status, suggesting a residual batch effect not removed in the between-array normalization step. Nevertheless, an overall effect of *w*MelPop on host gene expression was still distinguishable by the second principal component, which comprised 14% of the total variance, allowing the identification of 13 up- and 30 downregulated GO terms (**S3 Table**).

Results were widely consistent with the immune activation previously reported by Kambris et al. (2009), as top 10 upregulated GO terms Serine-type endopeptidase activity, Extracellular region and Carbohydrate binding (**Fig 1.C**) were driven by the overexpression of CLIPs, pattern recognition receptors, prophenoloxidases and defensins (**S3 Table**). Our analysis further revealed effects of *w*MelPop in host transport processes (**Fig 1.C**) not reported in the original publication, suggesting an impact of *w*MelPop on amino acid homeostasis (including four amino acid transporters), transition metal homeostasis (including transporters of iron, zinc and copper), intercompartmental pH balance (comprising four vacuolar ATP synthase subunits) and neuronal signaling (including neurotransmitter receptors and ion channels) (**S3 Table**).

Top 10 downregulated GO terms (**Fig 1.C**) suggested that *w*MelPop modulates RNA post-transcriptional modification patterns, with underexpression of putative ribonucleases, splicing factors, tRNA-methyltransferase, a nuclear cap-binding protein and a pre-mRNA cleavage factor involved in mRNA polyadenylation **(S3 Table)**. The results also hinted at a coordinated suppression of key elements for cell cycle regulation and DNA metabolism. Indeed, downregulation of GO terms Chromosome, Cell cycle **(Fig 1.C)** and DNA metabolic process **(S3 Table)** was driven by the underexpression of histone proteins, DNA damage checkpoint protein, DNA replication licensing factor, DNA methyltransferase, replication factor C subunit,

centromere/kinetochore protein, CDK (cyclin-dependent kinase) activating kinase and CDK activating kinase assembly factor, among others (**S3 Table**).

Rancès et al. (2012)

Rancès et al. (2012) aimed to identify immune genes involved in *Wolbachia*'s pathogen blocking in *A. aegypti*, comparing whole-body transcriptome of female *w*MelPop- and *w*Mel-infected mosquitoes (lines PGYP1 and MGYP2) versus their tetracycline-treated counterparts (lines PGYP1.tet and MGYP2.tet). 12 two-channel Agilent microarray slides were competitively hybridized to *Wolbachia*-infected and uninfected cDNA samples (6 for PGYP1 vs PGYP1.tet and 6 for MGYP2 vs MGYP2.tet), each sample derived from an independent pool of twenty 8-days-old mosquitoes. Genespring v9.0 software was used for normalizing intensity data and conducting differential expression analysis, defining DEGs as those with FDR q-value ≤ 0.05 and absolute fold-change ≥ 1.5. Upregulated genes were subjected to overrepresentation analysis against the distribution of GO categories for the *A. aegypti* genome [27]. Our *de novo* analysis of this dataset (**Fig 2**) complemented the identification of upregulated functions and provided an unprecedented identification of downregulated functions.

Fig 2. Transcriptomic effects of *w*MelPop and *w*Mel on female *A. aegypti* whole bodies assessed from the analysis of the dataset in Rancès et al. (2012). (A) PCA of normalized log-intensities. (B) Hierarchical biclustering of z-scores from normalized log-intensities. Column names denote slides and channels, with R for red and G for green. (C) Top 20 GSEA results for the *w*MelPop comparison (left) and the *w*Mel comparison (right).

Results showed a strong transcriptomic effect of both infection status and *Wolbachia* strain (**Fig 2.A and 2.B**), with a stronger overall effect of *w*MelPop than *w*Mel (**Fig 2.A)**. This was depicted as the separation of infected and uninfected samples according to PC1 was more pronounced for *w*MelPop, which is consistent with a larger number of DEGs reported by Rancès et al. (2012) for that strain. In total, 27 up- and 30 downregulated GO

terms were found here for *w*MelPop-infected *A. aegypti* and 5 up- and 10 downregulated GO terms for *w*Mel-infected *A. aegypti* (**S3 Table**).

Our results were consistent with the immune activation reported by Rancès et al. (2012), as top 10 upregulated GO terms Serine-type endopeptidase activity and Extracellular region (**Fig 2.C left and right**) reflected the overexpression of CLIPs, serine protease inhibitors, transferrin and defensin, as well as prophenoloxidases in the case of *w*MelPop (**S3 Table**). Upregulation of Electron transport chain and Respirasome (**Fig 2.C, left**) was also consistent with the upregulation of Electron carrier activity reported by the authors.

As in the original analysis by Rancès et al. (2012), we found that *w*MelPop upregulates transmembrane transport (**Fig 2.C, left**), with underlying upregulation of amino acid transporters, synaptic vesicle proteins, glutamate and sugar transporters, vacuolar ATPases and ion channels (**S3 Table**). However, we found that this broad effect on transport functions is not restricted to *w*MelPop, as *w*Mel upregulated Salt transmembrane transporter activity (**Fig 2.C, right**), comprising amino acid transporters, ion channels, calcium-transporting ATPase and mitochondrial carrier proteins (**S3 Table**).

Our analysis of downregulated genes suggested disruption of DNA replication and cell cycle by both *w*Mel and *w*MelPop, which was not identified in the original study. Top 10 downregulated terms Cell cycle and Chromosome (**Fig 2.C, left and right**) reflected underexpression of DNA polymerase subunits, DNA repair proteins, DNA helicases, anaphase-promoting complex subunits, M-phase inducer phosphatase and a putative cyclin **(S3 Table)**. For *w*MelPop, downregulation of these terms was further driven by additional cyclins, CDK, CDK activating kinase and a CDK regulatory subunit **(S3 Table)**. *w*MelPop also downregulated RNA processing (**Fig 2.C, left**), with underexpression of ribonucleases, ribonucleoproteins, RNA methyltransferases, splicing factors and cap-binding protein subunits (**S3 Table**); as well as microtubule-mediated transport (**Fig 2.C, left**), with underexpression of tubulin chains, katanin P80 subunit, gamma-tubulin complex component, kinesin and dynein chains (**S3 Table**).

Ye et al. (2013)

Ye et al. (2013) characterized the methylome of female *w*MelPop-infected and uninfected *A. aegypti* (lines PGYP1 and PGYP1.tet) heads and muscles, examining its relationship with gene expression changes. 12 two-channel Agilent microarrays were competitively hybridized to PGYP1 and PGYP1.tet cDNA samples (6 for heads and 6 for muscles), each sample derived from a pool of 20 heads or muscle tissues. Intensity data was normalized with the *lowess* method and differential expression analyses were conducted using a cross-gene error model and FDR *q*-value to correct for multiple testing [28]. Differential expression analysis was used to search for correlations between gene methylation and expression across conditions, however, no functional characterization of the genome-wide expression patterns was performed [28]. We analyzed this dataset to identify the main functional effects of *w*MelPop in *A. aegypti*'s heads and tissues (**Fig 3**).

Fig 3. Transcriptomic effects of *w*MelPop on female *A. aegypti* muscles and heads assessed from the analysis of the dataset in Ye et al. (2013). (A) PCA of normalized log-intensities. (B) Hierarchical biclustering of z-scores from normalized log-intensities. Column names denote slides and channels, with R for red and G for green. (C) Top 20 GSEA results for the muscle comparison (left) and the head comparison (right).

PCA and hierarchical clustering of transcriptomic profiles (**Fig 3.A** and **Fig 3.B**) showed that tissue was the main factor influencing global gene expression in this dataset. Still, the effect of *w*MelPop was distinguishable from the PCA, where infected and uninfected samples were segregated by the PC2, which accounted for 12% of the total variance. In total, we found 6 up- and 12 downregulated GO terms in *w*MelPop-infected muscles and 9 up- and 4 downregulated GO terms in *w*MelPop-infected heads (**Fig 3.C, left and right**).

Infected muscles showed upregulation of Serine-type endopeptidase activity, Extracellular region and Carbohydrate binding, and downregulation of RNA processing (**Fig 3.C, left**), which was consistent with our analyses presented previously for *w*MelPop-infected whole bodies (**Fig 1.C** and **Fig 2.C, left**). Our results also suggested a disruption of aerobic energy metabolism in muscles, with downregulation of the GO term

Mitochondrion (**Fig 3.C, left**), driven by the underexpression of NADH dehydrogenases, ATP synthase components, mitochondrial pyruvate carrier and mitochondrial ribosomal proteins, among others **(S3 Table)**.

Infected head tissues exhibited an increased demand for protein synthesis due to *w*MelPop, with upregulation of tRNA metabolism (**Fig 3.C, right**) driven by overexpression of aminoacyl-tRNA synthetases for 13 of the 20 standard amino acids, among others **(S3 Table)**. We also found that *w*MelPop downregulated G protein-coupled receptor (GPCR) signaling pathway in *A. aegypti* heads (**Fig 3.C, right**), including underexpression of G-protein subunits, neuropeptides and several GPCRs including 6 long and short wavelength opsins **(S3 Table)**. Downregulation of these genes may have profound impacts for diverse insect physiological processes regulated by GPCRs, such as reproduction, neurotransmission and stress responses. Particularly, downregulation of opsins, which are integral membrane components that mediate phototransduction, may impair light sensitivity and thus impact mosquito light-driven behavior [55,56].

Wimalasiri-Yapa et al. (2023)

Wimalasiri-Yapa et al. (2023) studied the temporal progression of *A. aegypti*'s transcriptional response to *Wolbachia* in field conditions, considering Australian mosquito populations that were subjected to *w*Mel releases in 2011, 2013/2014 and 2017 (hereafter, the "2011-, 2014- and 2017-infected populations") and an uninfected population. Illumina NovaSeq6000 reads were used to compare the whole-body transcriptome of *w*Mel-infected female mosquitoes with each release history versus the uninfected population. The 2011-, 2014- and 2017-infected populations and the uninfected one were represented by 12, 9, 7 and 5 independent samples, respectively, each one consisting in a pool of five 4-days-old females. Reads were mapped to the AaegL5 reference genome and counts were subjected to differential expression analyses with DESeq2, defining DEGs as those with FDR<0.05 and absolute log2 fold change>1. The DAVID software was used for annotation, clustering and enrichment analyses of functional categories in DEG sets [31]. Our analysis (**Fig 4**) offered complementary insights into the functional changes induced by *w*Mel in wild *A. aegypti* populations.

Fig 4. Temporal progression of *w*Mel transcriptomic effects on native *A. aegypti* populations assessed from the analysis of the dataset in Wimalasiri-Yapa et al. (2023). (A) PCA of normalized log-intensities. (B) Hierarchical biclustering of z-scores from normalized log-intensities. (C) Top 20 GSEA results for the 2011-infected (left), 2014-infected (middle) and 2017-infected (right) populations.

Both PCA (**Fig 4.A**) and hierarchical clustering of transcriptomic profiles (**Fig 4.B**) grouped uninfected samples together. PC1, which accounted for 41% of the total variance, segregated uninfected from infected samples, with the greatest distance being between most recent introgression (2017) and the uninfected status. This was consistent with the highest number of DE genes being found for the 2017-infected population in the original publication. The total number of up/downregulated GO terms found was 30/28 for the 2011-infected population, 35/33 for the 2014-infected population and 49/36 for the 2017-infected population (**S3 Table**).

Upregulation of Serine hydrolase activity and Endopeptidase inhibitor activity in all infected populations **(Fig 4.C)** was consistent with the results of Wimalasiri-Yapa et al. (2023). Also, upregulation of Organic acid biosynthetic process **(Fig 4.C)**, driven by overexpression of several genes implicated in fatty acid biosynthesis (**S3 Table**), was consistent with the enrichment of Fatty acid biosynthetic process reported by the authors for all populations. Our results further indicated enhancement of host aerobic respiration by *w*Mel (**Fig 4.C**) in all infected populations, which was not identified in the original publication and was driven by upregulation of succinate dehydrogenase, cytochromes, ATP synthase components and NADH dehydrogenases, among others (**S3 Table**).

GO terms that were among the top 10 downregulated in all comparisons were in concordance with the original analysis of Wimalasiri-Yapa et al. (2023), denoting a disruption of cell cycle and DNA metabolic processes (**Fig 4.C**), driven by downregulation of cyclins, DNA replication licensing factors, endonucleases, DNA polymerase components, DNA topoisomerase, origin recognition complex subunit, DNA mismatch repair protein and DNA helicase, among others (**S3 Table**).

Boehm et al. (2023)

Boehm et al. (2023) studied the transcriptomic effects of *w*Mel on *A. aegypti* carcasses and midguts at different times post-blood feeding and with different status of ZIKV infection. We limit the following description to what concerns the experiments without viral infection. Illumina NovaSeq reads were used to compare the carcass and midgut transcriptomes of *w*Mel-infected and uninfected female mosquitoes at 4 or 7 days post-feeding (dpf). Each combination of time post-feeding, tissue and *Wolbachia* status was represented by 3 biological replicates, each one comprising 30 midguts or carcasses. Reads were aligned to the *A. aegypti* reference genome AaegL5.3 using a pseudo-alignment approach, counts were summarized at the gene level and subjected to differential expression analyses with DESeq2. DEGs were defined as those with FDR < 0.01 and absolute base-2 logarithmic fold change > 1. GSEA was performed on normalized data against five lists of *A. aegypti* gene sets that were curated from previous genomic and transcriptomic studies [30]. In the following we present the results of our own analysis of this dataset (**Fig 5**).

Fig 5. Transcriptomic effects of *w*Mel on female *A. aegypti* carcasses and midguts at different times post blood feeding assessed from the analysis of the dataset in Boehm et al. (2023). (A) PCA of normalized log-intensities. (B) Hierarchical biclustering of z-scores from normalized log-intensities. (C) Top 20 GSEA results for the carcass at 4 dpf (up, left), carcass at 7 dpf (up,right), midgut at 4 dpf (down, left) and midgut at 7dpf (down, right).

PCA (**Fig 5.A**) and hierarchical biclustering (**Fig 5.B**) posed tissue as the main grouping factor, separating samples along the PC1, which explained 88% of the total variance. PC2 distinguished infected from uninfected carcasses, while for midguts the distinction according to infection status was less clear. Time post feeding appeared as the least impacting factor on global gene expression profiles. The total number of up/downregulated GO terms found was 13/1 for carcass at 4dpf, 11/0 for carcass at 7dpf, 11/4 for midguts at 4 dpf, and 14/2 for midguts at 7 dpf (**Fig 5.C**).

Results denoted common upregulation of respirasome (**Fig 5.C**), driven by the overexpression of cytochromes c, cytochromes c oxidases and NADH dehydrogenases, among others (**S3 Table**), which was consistent with the original publication. Our results went one step further showing a common upregulation of ribosomal components (**Fig 5.C**), with overexpression of several 40S, 60S and mitochondrial ribosomal proteins (**S3 Table**), representing new functional insights that were not obtained in the original analysis.

Top 10 downregulated genes for carcasses and midguts at 4 dpf denoted suppression of nuclear functions **Fig 5.C up, left and down, left)**, which was driven by the underexpression of genes related to DNA metabolism, RNA transcription and processing, chromosome maintenance and cell cycle regulation (**S3 Table**). This was consistent with the downregulation of GO terms Nucleus and Chromosome reported by Boehm et al. (2023) for these conditions. In midguts at 7 dpf we found downregulation of Extracellular region and Serine hydrolase activity (**Fig 5.C, down, right**), explained by the underexpression of serine-type peptidases and several other extracellular genes such as serine protease inhibitors, thrombospondin, prophenoloxidase and lipases (**S3 Table**). The downregulation of Extracellular region and Serine hydrolase activity was consistent with the original results of Boehm et al. (2023) for midguts at 7 dpf, however, it contrasted with our analysis of all previous datasets, where these GO terms were always upregulated (**S3 Table**).

Consistent transcriptomic effects of *Wolbachia* in *Aedes aegypti*

In order to find functions consistently affected by *Wolbachia* on its host, *p*-values derived from individual differential expression and GSEA tests were combined using the maxP approach (see Methods), finding 1,483 and 57 significant genes and GO terms, respectively (**S4 Table**). This set was further constrained to focus on genes that: (i) had a consistent direction of differential expression across tests (*i.e.*, logarithmic fold-change always positive or negative), and (ii) were individually significant ($p<0.05$) in at least 8 of the 12 differential expression tests. Genes fulfilling these conditions were called consistently up- or downregulated genes (**Tables 2 and 3**, respectively). We applied a similar criterion for finding consistently up- or downregulated functions but, given that no significant GO term was always up- or downregulated, we required at least 10 tests with the same regulation direction (**Table 4**).

Table 2. Genes consistently upregulated by *Wolbachia* in *Aedes aegypti*

Gene ID	Mean Fold-change[a]	# significant tests (p<0.05)	Description	Category
AAEL001508	4.0 ± 1.9	11/12	InterPro: Farnesoic acid O-methyltransferase	Metabolism
AAEL004667	3.1 ± 1.5	11/12	InterPro: Farnesoic acid O-methyltransferase	
AAEL000829	1.3 ± 0.2	11/12	Dimethylaniline monooxygenase. InterPro: Flavin monooxygenase FMO	
AAEL004278	2.7 ± 1.2	11/12	GO: Lipid metabolic process, Integral component of membrane, Oxidoreductase activity, Heme binding	
AAEL000024	1.9 ± 0.8	10/12	Dopachrome-conversion enzyme, putative	
AAEL014246	1.5 ± 0.3	9/12	Glucosyl/glucuronosyl transferases	
AAEL003832	11.7 ± 6.7	11/12	Defensin anti-microbial peptide (*DEFC*)	Innate immunity
AAEL015458	14.4 ± 12.1	11/12	Transferrin (*Tf1*)	
AAEL011453	2.8 ± 1.1	10/12	C-Type Lectin (*CTL14*)	
AAEL011621	2.8 ± 1.1	10/12	C-Type Lectin - mannose binding (*CTLMA13*)	
AAEL009474	3.1 ± 1.5	10/12	Peptidoglycan Recognition Protein (Short) (*PGRPS1*)	
AAEL006516	1.3 ± 0.2	10/12	Vacuolar ATP synthase subunit h	Trans-membrane transport
AAEL010819	1.3 ± 0.2	9/12	Vacuolar ATP synthase subunit H	
AAEL000291	1.2 ± 0.1	9/12	V-type proton ATPase 16 kDa proteolipid subunit	
AAEL010139	16.9 ± 28.8	11/12	Serine protease, putative	Proteolysis
AAEL013032	2.2 ± 1.3	10/12	GO: Serine-type endopeptidase activity, Proteolysis. InterPro: Trypsin_dom	
AAEL003963	1.4 ± 0.2	9/12	Calpain 4, 6, 7, invertebrate	
AAEL001082	1.8 ± 0.6	10/12	InterPro: Myofilin (IPR031828)	Other
AAEL006507	1.5 ± 0.3	9/12	GO: Methyltransferase activity. InterPro: RNA methyltransferase Bin3-like	
AAEL008471	1.4 ± 0.2	9/12	GO: Protein targeting, Intracellular protein transport, ATP binding. InterPro: SecA	
AAEL003417	1.4 ± 0.2	9/12	Mitochondrial ATPase inhibitor, putative	

[a] Mean Fold-changes ± Standard Deviation. The reference condition for Fold-change calculation is *Wolbachia*-uninfected.

Table 3. Genes consistently downregulated by *Wolbachia* in *Aedes aegypti*

Gene ID	Mean Fold-change[a]	# significant tests (p<0.05)	Description	Category
AAEL014016	1.2 ± 0.1	9/12	Breast cancer metastasis-suppressor. InterPro: Sds3-like	Nucleic acid interaction
AAEL012392	1.3 ± 0.2	8/12	GO: Nucleus, Nucleic acid binding, Zinc ion binding	
AAEL010797	1.2 ± 0.1	8/12	Mediator of RNA polymerase II transcription subunit 21 (Med21)	
AAEL003490	1.3 ± 0.2	8/12	Zinc finger-tcix domain-containing protein	
AAEL009650	1.3 ± 0.2	8/12	GO: Nucleic acid binding, 3'-5' exonuclease activity	

AAEL012989	1.2 ± 0.1	8/12	Nuclear pore complex protein Nup85	
AAEL014347	1.3 ± 0.2	8/12	GO: Integral component of membrane, Calcium ion binding, Protein binding	
AAEL004308	1.1 ± 0.1	8/12	Proteasome subunit alpha type	Other
AAEL014816	1.3 ± 0.2	8/12	Uncharacterized product	
AAEL012148	1.6 ± 0.6	8/12	Uncharacterized product	

[a] Mean Fold-changes ± Standard Deviation. The reference condition for Fold-change calculation is *Wolbachia*-infected.

Table 4. GO terms consistently up- and downregulated by *Wolbachia* in *Aedes aegypti*

Category	GO terms	Expression pattern
Electron transport chain	Respirasome, Respiratory chain complex, Oxidoreduction-driven active transmembrane transporter activity, Oxidative phosphorylation, ATP synthesis coupled electron transport, Respiratory electron transport chain, Electron transfer activity, Mitochondrial inner membrane, Mitochondrial respirasome, Aerobic electron transport chain, Mitochondrial ATP synthesis coupled electron transport, Oxidoreductase complex.	Upregulated in all infected groups except for *w*MelPop-infected heads and muscles from Ye et al. (2013).
Carbohydrate transmembrane transport	Carbohydrate transmembrane transporter activity, Sugar transmembrane transporter activity, Carbohydrate transmembrane transport.	Upregulated in all infected groups except for *w*MelPop-infected heads and muscles from Ye et al. (2013).
Serine-type peptidase activity	Serine hydrolase activity, Serine-type peptidase activity, Serine-type endopeptidase activity	Upregulated in all infected groups except for *w*Mel-infected midguts from Boehm et al. (2023).
Serine-type peptidase inhibition	Serine-type endopeptidase inhibitor activity, Negative regulation of catalytic activity, Negative regulation of molecular function, Negative regulation of protein metabolic process	Upregulated in all infected groups except for *w*Mel-infected midguts from Boehm et al. (2023).
DNA replication	DNA replication	Downregulated in all infected groups except for *w*MelPop-infected heads and muscles from Ye et al. (2013).

We found 21 consistently upregulated genes related to metabolism, innate immunity, transmembrane transport, proteolysis and other functions (**Table 2**). Metabolism-related genes included two putative farnesoic acid O-methyltransferases, involved in the synthesis of juvenile hormones [57], a flavin-dependent monooxygenase, involved in detoxification [58] and a putative dopachrome conversion enzyme, involved in melanin biosynthesis [53]. Innate immunity-related genes comprised two C-type lectins and a PGRP, which are pathogen pattern recognition genes, as well as the extracellular iron transporter transferrin which serves immune functions by limiting pathogen access to iron [59], and the antimicrobial peptide defensin. Transmembrane transport genes comprised three subunits of vacuolar ATP synthase, which is a proton pump responsible for the acidification of intracellular organelles [60]. Additional genes included a putative mitochondrial ATPase inhibitor, a putative RNA-methyltransferase and myofilin, which is a component of the

thick filaments of insect striated muscles [61].

We also found 10 consistently downregulated genes (**Table 2**) mainly related to nucleic acid interaction, including a Sds3-like gene (which are implicated in repression of gene expression [53]), Med21 (a component of the Mediator of transcriptional regulation, which mediates the interaction of RNA polymerase II and transcription activators or repressors [62]), and a putative RNA-exonuclease. Additional genes included a nuclear pore protein, a proteasome subunit and two genes with uncharacterized function.

Consistently upregulated GO terms were associated to the electron transport chain, carbohydrate transmembrane transport, serine-type peptidase activity and serine-type peptidase inhibition, while the GO term DNA replication was consistently downregulated (**Table 3**).

Discussion

Although *Wolbachia pipientis* is currently being used for arboviral disease control, a robust mechanistic understanding of the *A. aegypti*-*Wolbachia* system is still lacking. Our analysis provides new insights on previously published transcriptomic datasets and identifies host genes and functions commonly affected by *Wolbachia* transinfection, transcending differences such as tissue, age and bacterial strain, thus providing a crucial resource that could impact strategies to enhance and preserve the efficacy of this arboviral disease control approach.

New functional insights on the effects of *Wolbachia* in *A. aegypti*

De novo analyses performed in this work revealed functional impacts of *Wolbachia* transfection in *A. aegypti* that were concealed within published datasets. These included upregulation of transport processes in data from [25], downregulation of cell cycle and DNA metabolism in [25] and [27], and upregulation of respirasome in [30]. The analysis of the dataset from Ye et al. (2013) is of particular interest as it comprises the only genome-wide transcriptomic data of *w*MelPop-infected *A. aegypti* heads published so far, posing it as a unique source of

tissue-specific mechanistic insight. We found that *w*MelPop downregulated six long and short wavelength opsins, light sensitive receptors that initiate phototransduction and mediate visual perception in mosquitoes from larval to adult stages [63,64]. A coordinated downregulation of opsins has been previously identified for the native *Wolbachia* infection of *Aedes fluviatilis* [14], but not for *A. aegypti* transinfection.

It has been shown that *w*MelPop attenuates photofobicity (*i.e.*, light avoidance) in *A. aegypti* larvae [65] and that inhibition of opsins impairs visual recognition of feeding targets in adult *A. aegypti* [55]. Considering these reports in the light of our findings, we propose downregulation of opsins as a feasible mechanism for photofobicity attenuation by *w*MelPop and predict that this strain impairs *A. aegypti*'s feeding target seeking. As photophobicity and feed seeking ability are relevant for mosquito fitness at multiple developmental stages —the first one reducing predation and desiccation risk for larvae [56] and the second one allowing adult females to obtain blood meals [55]— testing these hypotheses will help clarify mechanistic bases of the dramatic fitness costs induced by *w*MelPop, which hinder its use for population replacement [66].

Wolbachia consistently upregulates electron transport chain genes in *A. aegypti*

Several GO terms associated with host electron transport chain (ETC) and carbohydrate transmembrane transport were found to be upregulated by *Wolbachia* in 10 out of the 12 analyzed datasets. ETC is a central step in mitochondrial aerobic respiration, responsible for most of adenosine triphosphate (ATP) production in the cell and is fueled by glycolysis of carbohydrates. Upregulation of host ETC and carbohydrate transmembrane transport can be interpreted as a tendency to increase ATP production along with the availability of sugars to fuel this process. Consistent upregulation of the putative mitochondrial ATPase inhibitor *AAEL003417* also identified in this work may be a compensatory mechanism to control ATP production.

While it has been suggested that *Wolbachia* provides hosts with ATP from its own bacterial aerobic respiration [67,68], to the best of our knowledge our study is the first to show the persistence of host ETC upregulation by

Wolbachia in *A. aegypti*. Interestingly, *Wolbachia* has a complete biosynthetic pathway for heme synthesis and may provide it to its hosts [67]. As ETC heavily depends on heme, it could be hypothesized that *Wolbachia* further supports host ETC upregulation by providing this cofactor.

Upregulation of ETC can also be linked to *Wolbachia*'s induction of reactive oxygen species (ROS) in *Aedes* hosts [26,69,70], which is considered a key phenomenon for antiviral defense in *Diptera* [26,69,71,72]. Electron leakage, which is an incomplete reduction of oxygen to form superoxide (O_2^-) due to ETC activity, is a major source of cellular ROS [73]. We propose that a generalized upregulation of ETC genes is a potential persistent host mechanism behind ROS induction by *Wolbachia* in *A. aegypti*. Additionally, as the extent of electron leakage is modulated by mitochondrial ATPase activity [73,74], the consistent upregulation of putative mitochondrial ATPase inhibitor *AAEL003417* found here might be further modulating ROS production.

It has been previously proposed that the main *A. aegypti* factors responsible for *Wolbachia*-induced ROS are dual oxidases and NADPH-oxidases [26,75], which drive an immune oxidative burst in *Drosophila* under microbial infection [76]. Surprisingly, we found that NADPH-oxidase *AAEL002039* was insignificant (p>0.05) in 11 of 12 tests, while all six significant results for dual oxidase *AAEL007563* and its maturation factor *AAEL007562* corresponded to downregulation (**S4 Table**). Typical downregulation of *AAEL007562* and *AAEL007563* could constitute a host mechanism to counterbalance oxidative stress associated with other mechanisms such as the bacterial aerobic respiration and, as previously discussed, host ETC upregulation.

Our results contrast with the 28-fold increase in *AAEL007562* transcripts reported by Pan et al. (2012) for *w*AlbB-infected carcasses of non-blood fed *A. aegypti* [26], a discordance that may be attributed to the difference of *Wolbachia* strains or specific biological conditions. On the other hand, our results are consistent with the study of Caragata et al. (2016) on *w*Mel-infected *A. aegypti* whole bodies, where ROS induction was verified without upregulation of *AAEL007562* [70] and further supports an alternative mechanism for typical ROS production such as enhanced host ETC activity. This does not exclude the possibility that dual- and NADPH-oxidases plays a role in pathogen blocking by producing ROS early after a blood meal, which may have been missed in the transcriptomic datasets from Boehm et al. (2023) at 4 and 7 days post blood feeding

analyzed in this work.

Wolbachia consistently upregulates vacuolar ATP synthase subunits in *A. aegypti*

We found three consistently upregulated vacuolar ATP synthase (v-ATPase) subunits: *AAEL006516*, *AAEL010819* and *AAEL000291*. v-ATPases are proton pumps that acidify intracellular membranous organelles, such as lysosomes, endosomes and parasitophorous vacuoles [60]. As *Wolbachia* lives inside host-derived vacuoles [77,78], consistent upregulation of v-ATPases may have direct impacts in the immediate environment of the bacteria.

v-ATPases are also responsible for the acidification of DENV-containing endosomes, which is a requisite for the release of viral RNA into the cytoplasm for further translation and replication. Consequently, inhibition of v-ATPases has proven antagonistic to DENV infection in *Aedes* mosquitoes, *Aedes* cells and *HeLa* cells [79–81]. Therefore, v-ATPase upregulation may be a pro-viral effect of *Wolbachia*, obscured however by its repertoire of antiviral effects. Existence of pro-viral *Wolbachia* effects should be carefully considered, as overall enhancement of arbovirus infection by *Wolbachia* is possible [82]. Specifically, disruption of v-ATPase activity by RNAi or v-ATPase inhibitors hold potential to clarify the consequences of *Wolbachia*'s upregulation of host v-ATPases for viral infection in *A. aegypti*.

Wolbachia consistently upregulates two putative farnesoic acid methyl transferases in *A. aegypti*

We found the consistent upregulation of two putative farnesoic acid methyl transferases (FAMeTs), *AAEL001508* and *AAEL004667*, which catalyze the conversion of farnesoic acid to methyl farnesoate, a late step in the biosynthesis of insect juvenile hormones [89,90]. Interactions of *Wolbachia* with the juvenile hormone biosynthetic pathway have been previously reported in *Diptera* [83,84], but to the best of our knowledge, this is the first study showing *Wolbachia*'s consistent upregulation of putative *A. aegypti*'s

FAMeTs.

Juvenile hormone III (JHIII) is a key regulator of development and reproduction in *A. aegypti*, and its titer determines the expression of thousands of genes [83,85,86]. Also, the direct product of FAMeT —methyl farnesoate— can partially substitute the functions of JHIII in *A. aegypti* [87] and possibly serve additional uncharacterized functions [88]. In light of these considerations, either by altering juvenile hormone or methyl farnesoate production, upregulation of FAMeTs could have deep consequences for *A. aegypti* physiology. Further experiments are needed to confirm the enzymatic activity of *AAEL001508* and *AAEL004667*, as well as to unveil their specific roles in the *A. aegypti*-*Wolbachia* symbiosis at different life stages. Checking if this phenomena has a parallel in male mosquitoes would be of particular interest, as alterations of JHIII have been proposed as a contributory mechanism for *Wolbachia*-induced CI in *Drosophila* [83].

Wolbachia consistently upregulates a flavin-containing monooxygenase implicated in xenobiotic metabolism in *A. aegypti*

We found the consistent upregulation of flavin-containing monooxygenase (FMO) *AAEL000829*, which catalyzes the incorporation of an oxygen atom from O_2 to a compound, using flavin adenine dinucleotide as a prosthetic group [89,90]. Another FMO, *AAEL000834*, shows a similar profile of expression being upregulated in 8 of the 9 significant tests ($p<0.05$) (**S4 Table**). FMOs catalyze the oxygenation of nucleophilic nitrogen, sulphur, phosphorus and selenium atoms [53], and are implicated in the neutralization of xenobiotics (i.e. foreign substances) [58], particularly insecticides [89,91,92]. Although direct effects of *Wolbachia* on *A. aegypti*'s resistance to typical insecticides is not clear [93], the consistent upregulation of FMOs found here opens the question if there are additional substances to which *Wolbachia*-infected *A. aegypti* is more resistant than its uninfected counterpart.

Coordinating *Wolbachia*- and insecticide-based vector control methods is important for the overall success of arboviral control [21,94]. Particularly, coupling *Wolbachia*-introduction with that of insecticide resistance genotypes has been proposed as a way to facilitate spread of the bacteria in native mosquito populations, a

paramount task for the use of strains that cause high fitness costs such as *w*MelPop [21,94]. If the consistent upregulation of FMOs confers resistance to specific compounds in *Wolbachia*-infected *A. aegypti*, their controlled use might be considered to enhance *Wolbachia* introgression in native *A. aegypti* populations. By leveraging an effect already present in *Wolbachia*-infected *A. aegypti*, such a measure could avoid the introduction of new insecticide-resistant alleles in native populations, which is a major concern regarding the use of insecticides for the enhancement of *Wolbachia*-based arboviral control [21,94].

Wolbachia consistently downregulates genes with nucleic acid-related functions in *A. aegypti*

We found the GO term DNA replication downregulated by *Wolbachia* in 10 out of 12 tests. Together with the consistent upregulation of ETC and carbohydrate transmembrane transport, our results suggest a coordinated host metabolic shift towards enhanced aerobic energy metabolism and reduced cellular proliferation. This scenario may be induced by *Wolbachia* to favor its own preservation in *A. aegypti* adult stages such as those considered in this study, however, it is foreseeable that a similar effect in earlier developmental stages would critically impact development. It would be therefore interesting to study if this downregulation also stands in earlier stages of *A. aegypti* development, pinpointing the need for genome-wide transcriptomic analyses of *Wolbachia*-infected *A. aegypti* at new biological conditions.

Our results suggest that downregulation of genes with nucleic acid interaction is not restricted to DNA but includes RNA-interacting genes. For instance, the GO term mRNA metabolic process had a negative Normalized Enrichment Score in 10 out of 12 tests, 7 of which were significant ($p<0.05$) (**S4 Table**). RNA viruses such as DENV, ZIKV and CHIKV have small genomes and heavily depend on host factors for the success of their life cycle, including various host RNA-interacting genes [80,95,96]. Under this consideration, downregulation of RNA-interacting genes by *Wolbachia* may underlie the broad-range of RNA viruses to which *Wolbachia* offers protection. Particularly, the consistently downregulated gene *AAEL009650* is homologous with *Drosophila* exonuclease-like *CG6744*, which contributes to DENV infection [80]. This poses *AAEL009650* as a concrete target of study for clarifying the link between downregulation of functions related to

nucleic acid interaction and pathogen blocking.

A consistent signature of immune priming by *Wolbachia* in *A. aegypti*

The consistent upregulation of defensin *DEFC*, transferrin *Tf1*, peptidoglycan recognition protein *PGRPS1* and GO terms related to serine-type peptidase activity and inhibition, are consistent with *Wolbachia*'s priming of the Immunodeficiency (IMD) and Toll pathways in *A. aegypti* [27]. Indeed, expression of the antimicrobial peptide defensin and the extracellular iron binding protein transferrin (the immunity function of which consists in reducing iron availability for pathogens [59]) is inducible by the Toll- and Immunodeficiency (IMD) pathways [59,97]. These pathways in turn can be activated extracellularly by the action of pattern recognition receptors such as *PGRPS1*, which elicit protease signaling cascades mediated by serine-type peptidases and serine-type peptidase inhibitors [98]. The expression pattern of *Rel2* observed here is also consistent with the activation of the IMD pathway, as it has a positive expression change in 10 out of 12 tests, 9 of which are significant ($p<0.05$) (**S4 Table**).

However, some genes of these pathways are downregulated. Particularly, for the Toll pathway, *TUBE* has a negative expression change in 9 out of 12 tests, 6 of which are significant ($p<0.05$), while *Rel1A* has a negative expression change in 7 out of 12 tests, 6 of which are significant ($p<0.05$) (**S4 Table**). *IKK1*, part of the IMD pathway, has a negative expression change in 10 out of 12 tests, 3 of which are significant ($p<0.05$) (**S4 Table**). This suggests that *Wolbachia* elicit transcriptomic mechanisms tending to decrease activation of Toll and IMD pathways, which however are overcome by other effects that promote such activation.

A role of the Janus Kinase/Signal Transducer Activators of Transcription (JAK/STAT) pathway in *Wolbachia*'s pathogen blocking has also been hypothesized [99], as components of this pathway were upregulated by *Wolbachia* in *Drosophila* [100], and this pathway restricts DENV in *A. aegypti* [101] and West Nile Virus in Culex mosquitoes [102]. We found that JAK/STAT activators (*DOME*, *HOP*, *STAT*) and inhibitors (*SOCS*, *PIAS1*) are mainly downregulated, as from the 26 significant tests that they accumulate ($p<0.05$), 23 correspond to downregulation (**S4 Table**). Again, this suggests that there are conflicting transcriptomic mechanisms

regarding immune priming by *Wolbachia*.

Knowing the specific mechanisms underlying *Wolbachia*'s immune priming is crucial for understanding pathogen blocking by *Wolbachia* in *A. aegypti*, as it drives the expression of key antiviral factors such as *DEFC* [26] and transferrins [103]. Our work contributes in identifying consistent transcriptional regulations associated with immune priming by *Wolbachia* in *A. aegypti*. We also highlight that there are transcriptomic mechanisms opposing immune activation. These require careful consideration and monitoring, as they may constitute a basis for attenuation of pathogen blocking in the future, a main concern regarding *Wolbachia*-based arboviral control.

Conclusion

Genome-wide omic datasets from related conditions accumulate in time and bioinformatic resources enabling their interpretation evolve. This offers the opportunity to extract new value from previously published datasets by both analyzing them with up-to-date resources, and comparing older to newer datasets by meta-analysis methods, offering global insights that no study by its own can provide.

In this work, by performing a *de novo* meta-analysis of transcriptomic data we were able to identify novel effects and a transcriptomic signature of *Wolbachia* in *A. aegypti*, which can explain previously observed phenotypes and provide new hypotheses and gene targets. Particularly, *w*MelPop infected mosquitos display a coordinated downregulation of opsins in *A. aegypti* heads, which can be related to the loss of light sensitivity in mosquito larval stages that has been previously reported. We revealed *Wolbachia*'s consistent regulation of host genes that have escaped the focus of previous research, including a flavin-dependent monooxygenase and two farnesoic acid methyltransferases. We also highlight the common upregulation of functions associated with the electron transport chain, hypothesizing a role of this phenomena in pathogen blocking via induction of reactive oxygen species.

For this application, we note the relevance of availability of raw data, as identification of commonalities at the biological function level was mediated by gene set enrichment analyses that were not performed in the original publications, and that would not have been possible from pre-processed data. Follow-up work on our observations holds promise in producing valuable information towards the goals of preventing pathogen enhancement and loss of pathogen blocking, coupling *Wolbachia*-based control with other strategies, and enabling the use of specific *Wolbachia* strains, thus contributing towards the sustainability of *Wolbachia*-based arboviral control.

Acknowledgements

This research was funded by ANID, CMM FB210005, CeBiB PFBasal-0001 and NEMBICA STIC190013.

References

1. Dong B, Khan L, Smith M, Trevino J, Zhao B, Hamer GL, et al. Spatio-temporal dynamics of three diseases caused by Aedes-borne arboviruses in Mexico. Commun Med. 2022;2: 1–11. doi:10.1038/s43856-022-00192-7
2. Flores HA, O'Neill SL. Controlling vector-borne diseases by releasing modified mosquitoes. Nat Rev Microbiol. 2018;16: 508–518. doi:10.1038/s41579-018-0025-0
3. Jones R, Kulkarni MA, Davidson TMV, RADAM-LAC Research Team, Talbot B. Arbovirus vectors of epidemiological concern in the Americas: A scoping review of entomological studies on Zika, dengue and chikungunya virus vectors. PloS One. 2020;15: e0220753. doi:10.1371/journal.pone.0220753
4. Mariconti M, Obadia T, Mousson L, Malacrida A, Gasperi G, Failloux A-B, et al. Estimating the risk of arbovirus transmission in Southern Europe using vector competence data. Sci Rep. 2019;9: 17852. doi:10.1038/s41598-019-54395-5
5. Ogunlade ST, Meehan MT, Adekunle AI, Rojas DP, Adegboye OA, McBryde ES. A Review: Aedes-Borne Arboviral Infections, Controls and Wolbachia-Based Strategies. Vaccines. 2021;9: 32. doi:10.3390/vaccines9010032

6. Tajudeen YA, Oladunjoye IO, Mustapha MO, Mustapha ST, Ajide-Bamigboye NT. Tackling the global health threat of arboviruses: An appraisal of the three holistic approaches to health. Health Promot Perspect. 2021;11: 371–381. doi:10.34172/hpp.2021.48

7. Yen P-S, Failloux A-B. A Review: Wolbachia-Based Population Replacement for Mosquito Control Shares Common Points with Genetically Modified Control Approaches. Pathogens. 2020;9: 404. doi:10.3390/pathogens9050404

8. Zeng Z, Zhan J, Chen L, Chen H, Cheng S. Global, regional, and national dengue burden from 1990 to 2017: A systematic analysis based on the global burden of disease study 2017. eClinicalMedicine. 2021;32. doi:10.1016/j.eclinm.2020.100712

9. Kraemer MUG, Reiner RC, Brady OJ, Messina JP, Gilbert M, Pigott DM, et al. Past and future spread of the arbovirus vectors Aedes aegypti and Aedes albopictus. Nat Microbiol. 2019;4: 854–863. doi:10.1038/s41564-019-0376-y

10. Edenborough KM, Flores HA, Simmons CP, Fraser JE. Using Wolbachia to Eliminate Dengue: Will the Virus Fight Back? J Virol. 2021;95: e02203-20. doi:10.1128/JVI.02203-20

11. Ritchie SA, Hurk AF van den, Smout MJ, Staunton KM, Hoffmann AA. Mission Accomplished? We Need a Guide to the 'Post Release' World of Wolbachia for Aedes-borne Disease Control. Trends Parasitol. 2018;34: 217–226. doi:10.1016/j.pt.2017.11.011

12. Sim S, Ng LC, Lindsay SW, Wilson AL. A greener vision for vector control: The example of the Singapore dengue control programme. PLoS Negl Trop Dis. 2020;14: e0008428. doi:10.1371/journal.pntd.0008428

13. Caragata EP, Pais FS, Baton LA, Silva JBL, Sorgine MHF, Moreira LA. The transcriptome of the mosquito Aedes fluviatilis (Diptera: Culicidae), and transcriptional changes associated with its native Wolbachia infection. BMC Genomics. 2017;18: 6. doi:10.1186/s12864-016-3441-4

14. Dainty KR, Hawkey J, Judd LM, Pacidônio EC, Duyvestyn JM, Gonçalves DS, et al. wMel Wolbachia genome remains stable after 7 years in Australian Aedes aegypti field populations. Microb Genomics. 2021;7: 000641. doi:10.1099/mgen.0.000641

15. Raquin V, Moro CV, Saucereau Y, Tran F-H, Potier P, Mavingui P. Native Wolbachia from Aedes albopictus Blocks Chikungunya Virus Infection In Cellulo. PLOS ONE. 2015;10: e0125066.

doi:10.1371/journal.pone.0125066

16. Sigle LT, Jones M, Novelo M, Ford SA, Urakova N, Lymperopoulos K, et al. Assessing Aedes aegypti candidate genes during viral infection and Wolbachia-mediated pathogen blocking. Insect Mol Biol. 2022;31: 356–368. doi:10.1111/imb.12764

17. Utarini A, Indriani C, Ahmad RA, Tantowijoyo W, Arguni E, Ansari MR, et al. Efficacy of Wolbachia-infected mosquito deployments for the control of dengue. N Engl J Med. 2021;384: 2177–2186. doi:10.1056/NEJMoa2030243

18. Ryan PA, Turley AP, Wilson G, Hurst TP, Retzki K, Brown-Kenyon J, et al. Establishment of wMel Wolbachia in Aedes aegypti mosquitoes and reduction of local dengue transmission in Cairns and surrounding locations in northern Queensland, Australia. Gates Open Research; 2020. doi:10.12688/gatesopenres.13061.2

19. Pinto SB, Riback TIS, Sylvestre G, Costa G, Peixoto J, Dias FBS, et al. Effectiveness of Wolbachia-infected mosquito deployments in reducing the incidence of dengue and other Aedes-borne diseases in Niterói, Brazil: A quasi-experimental study. PLoS Negl Trop Dis. 2021;15: e0009556. doi:10.1371/journal.pntd.0009556

20. Bull JJ, Turelli M. Wolbachia versus dengue: Evolutionary forecasts. Evol Med Public Health. 2013;2013: 197–207. doi:10.1093/emph/eot018

21. Lindsey ARI, Bhattacharya T, Newton ILG, Hardy RW. Conflict in the Intracellular Lives of Endosymbionts and Viruses: A Mechanistic Look at Wolbachia-Mediated Pathogen-blocking. Viruses. 2018;10: 141. doi:10.3390/v10040141

22. Frentiu FD, Robinson J, Young PR, McGraw EA, O'Neill SL. Wolbachia-Mediated Resistance to Dengue Virus Infection and Death at the Cellular Level. PLOS ONE. 2010;5: e13398. doi:10.1371/journal.pone.0013398

23. Lu P, Bian G, Pan X, Xi Z. Wolbachia induces density-dependent inhibition to dengue virus in mosquito cells. PLoS Negl Trop Dis. 2012;6: e1754. doi:10.1371/journal.pntd.0001754

24. Moreira LA, Iturbe-Ormaetxe I, Jeffery JA, Lu G, Pyke AT, Hedges LM, et al. A Wolbachia Symbiont in Aedes aegypti Limits Infection with Dengue, Chikungunya, and Plasmodium. Cell. 2009;139: 1268–1278. doi:10.1016/j.cell.2009.11.042

25. Osborne SE, Iturbe-Ormaetxe I, Brownlie JC, O'Neill SL, Johnson KN. Antiviral Protection and the Importance of Wolbachia Density and Tissue Tropism in Drosophila simulans. Appl Environ Microbiol. 2012;78: 6922–6929. doi:10.1128/AEM.01727-12

26. Wimalasiri-Yapa BMCR, Huang B, Ross PA, Hoffmann AA, Ritchie SA, Frentiu FD, et al. Differences in gene expression in field populations of Wolbachia-infected Aedes aegypti mosquitoes with varying release histories in northern Australia. PLoS Negl Trop Dis. 2023;17: e0011222. doi:10.1371/journal.pntd.0011222

27. Weeks AR, Turelli M, Harcombe WR, Reynolds KT, Hoffmann AA. From Parasite to Mutualist: Rapid Evolution of Wolbachia in Natural Populations of Drosophila. PLOS Biol. 2007;5: e114. doi:10.1371/journal.pbio.0050114

28. Lindsey ARI, Bhattacharya T, Hardy RW, Newton ILG. Wolbachia and Virus Alter the Host Transcriptome at the Interface of Nucleotide Metabolism Pathways. mBio. 2021;12: e03472-20. doi:10.1128/mBio.03472-20

29. Baião GC, Schneider DI, Miller WJ, Klasson L. The effect of Wolbachia on gene expression in Drosophila paulistorum and its implications for symbiont-induced host speciation. BMC Genomics. 2019;20: 465. doi:10.1186/s12864-019-5816-9

30. Zheng Y, Wang J-L, Liu C, Wang C-P, Walker T, Wang Y-F. Differentially expressed profiles in the larval testes of Wolbachia infected and uninfected Drosophila. BMC Genomics. 2011;12: 595. doi:10.1186/1471-2164-12-595

31. Dou W, Miao Y, Xiao J, Huang D. Association of Wolbachia with Gene Expression in Drosophila Testes. Microb Ecol. 2021;82: 805–817. doi:10.1007/s00248-021-01703-0

32. He Z, Zheng Y, Yu W-J, Fang Y, Mao B, Wang Y-F. How do Wolbachia modify the Drosophila ovary? New evidences support the "titration-restitution" model for the mechanisms of Wolbachia-induced CI. BMC Genomics. 2019;20: 608. doi:10.1186/s12864-019-5977-6

33. Detcharoen M, Schilling MP, Arthofer W, Schlick-Steiner BC, Steiner FM. Differential gene expression in Drosophila melanogaster and D. nigrosparsa infected with the same Wolbachia strain. Sci Rep. 2021;11: 11336. doi:10.1038/s41598-021-90857-5

34. Rancès E, Ye YH, Woolfit M, McGraw EA, O'Neill SL. The Relative Importance of Innate Immune

Priming in Wolbachia-Mediated Dengue Interference. PLOS Pathog. 2012;8: e1002548. doi:10.1371/journal.ppat.1002548

35. Kambris Z, Cook PE, Phuc HK, Sinkins SP. Immune activation by life-shortening Wolbachia and reduced filarial competence in mosquitoes. Science. 2009;326: 134–136. doi:10.1126/science.1177531

36. Chung M, Basting PJ, Patkus RS, Grote A, Luck AN, Ghedin E, et al. A Meta-Analysis of Wolbachia Transcriptomics Reveals a Stage-Specific Wolbachia Transcriptional Response Shared Across Different Hosts. G3 GenesGenomesGenetics. 2020;10: 3243–3260. doi:10.1534/g3.120.401534

37. Edgar R, Domrachev M, Lash AE. Gene Expression Omnibus: NCBI gene expression and hybridization array data repository. Nucleic Acids Res. 2002;30: 207–210. doi:10.1093/nar/30.1.207

38. Parkinson H, Kapushesky M, Shojatalab M, Abeygunawardena N, Coulson R, Farne A, et al. ArrayExpress—a public database of microarray experiments and gene expression profiles. Nucleic Acids Res. 2007;35: D747–D750. doi:10.1093/nar/gkl995

39. R Core Team. R: A Language and Environment for Statistical Computing. R Foundation for Statistical Computing; 2022. Available: https://www.R-project.org/

40. Ritchie ME, Phipson B, Wu D, Hu Y, Law CW, Shi W, et al. limma powers differential expression analyses for RNA-sequencing and microarray studies. Nucleic Acids Res. 2015;43: e47. doi:10.1093/nar/gkv007

41. Smyth GK, Speed T. Normalization of cDNA microarray data. Methods San Diego Calif. 2003;31: 265–273. doi:10.1016/s1046-2023(03)00155-5

42. McCarthy DJ, Smyth GK. Testing significance relative to a fold-change threshold is a TREAT. Bioinformatics. 2009;25: 765–771. doi:10.1093/bioinformatics/btp053

43. Leinonen R, Sugawara H, Shumway M. The Sequence Read Archive. Nucleic Acids Res. 2011;39: D19–D21. doi:10.1093/nar/gkq1019

44. Afgan E, Baker D, Batut B, van den Beek M, Bouvier D, Čech M, et al. The Galaxy platform for accessible, reproducible and collaborative biomedical analyses: 2018 update. Nucleic Acids Res. 2018;46: W537–W544. doi:10.1093/nar/gky379

45. Andrews S. FastQC: a quality control tool for high throughput sequence data. 2010. Available: http://www.bioinformatics.babraham.ac.uk/projects/fastqc

46. Bolger AM, Lohse M, Usadel B. Trimmomatic: a flexible trimmer for Illumina sequence data. Bioinformatics. 2014;30: 2114–2120. doi:10.1093/bioinformatics/btu170

47. Dobin A, Davis CA, Schlesinger F, Drenkow J, Zaleski C, Jha S, et al. STAR: ultrafast universal RNA-seq aligner. Bioinformatics. 2013;29: 15–21. doi:10.1093/bioinformatics/bts635

48. dos Santos G, Schroeder AJ, Goodman JL, Strelets VB, Crosby MA, Thurmond J, et al. FlyBase: introduction of the Drosophila melanogaster Release 6 reference genome assembly and large-scale migration of genome annotations. Nucleic Acids Res. 2015;43: D690–D697. doi:10.1093/nar/gku1099

49. Gramates LS, Agapite J, Attrill H, Calvi BR, Crosby MA, dos Santos G, et al. FlyBase: a guided tour of highlighted features. Genetics. 2022;220: iyac035. doi:10.1093/genetics/iyac035

50. Liao Y, Smyth GK, Shi W. featureCounts: an efficient general purpose program for assigning sequence reads to genomic features. Bioinformatics. 2014;30: 923–930. doi:10.1093/bioinformatics/btt656

51. Love MI, Huber W, Anders S. Moderated estimation of fold change and dispersion for RNA-seq data with DESeq2. Genome Biol. 2014;15: 550. doi:10.1186/s13059-014-0550-8

52. Raghavan V, Kraft L, Mesny F, Rigerte L. A simple guide to de novo transcriptome assembly and annotation. Brief Bioinform. 2022;23: bbab563. doi:10.1093/bib/bbab563

53. Grabherr MG, Haas BJ, Yassour M, Levin JZ, Thompson DA, Amit I, et al. Full-length transcriptome assembly from RNA-Seq data without a reference genome. Nat Biotechnol. 2011;29: 644–652. doi:10.1038/nbt.1883

54. Simão FA, Waterhouse RM, Ioannidis P, Kriventseva EV, Zdobnov EM. BUSCO: assessing genome assembly and annotation completeness with single-copy orthologs. Bioinformatics. 2015;31: 3210–3212. doi:10.1093/bioinformatics/btv351

55. Li B, Dewey CN. RSEM: accurate transcript quantification from RNA-Seq data with or without a reference genome. BMC Bioinformatics. 2011;12: 323. doi:10.1186/1471-2105-12-323

56. Tang S, Lomsadze A, Borodovsky M. Identification of protein coding regions in RNA transcripts. Nucleic Acids Res. 2015;43: e78. doi:10.1093/nar/gkv227

57. Johnson M, Zaretskaya I, Raytselis Y, Merezhuk Y, McGinnis S, Madden TL. NCBI BLAST: a better web interface. Nucleic Acids Res. 2008;36: W5–W9. doi:10.1093/nar/gkn201

58. Giraldo-Calderón GI, Emrich SJ, MacCallum RM, Maslen G, Dialynas E, Topalis P, et al. VectorBase:

an updated bioinformatics resource for invertebrate vectors and other organisms related with human diseases. Nucleic Acids Res. 2015;43: D707–D713. doi:10.1093/nar/gku1117

59. Raudvere U, Kolberg L, Kuzmin I, Arak T, Adler P, Peterson H, et al. g:Profiler: a web server for functional enrichment analysis and conversions of gene lists (2019 update). Nucleic Acids Res. 2019;47: W191–W198. doi:10.1093/nar/gkz369

60. Hong G, Zhang W, Li H, Shen X, Guo Z. Separate enrichment analysis of pathways for up- and downregulated genes. J R Soc Interface. 2014;11: 20130950. doi:10.1098/rsif.2013.0950

61. Zdobnov EM, Kuznetsov D, Tegenfeldt F, Manni M, Berkeley M, Kriventseva EV. OrthoDB in 2020: evolutionary and functional annotations of orthologs. Nucleic Acids Res. 2021;49: D389–D393. doi:10.1093/nar/gkaa1009

62. Ye YH, Woolfit M, Huttley GA, Rancès E, Caragata EP, Popovici J, et al. Infection with a Virulent Strain of Wolbachia Disrupts Genome Wide-Patterns of Cytosine Methylation in the Mosquito Aedes aegypti. PLOS ONE. 2013;8: e66482. doi:10.1371/journal.pone.0066482

63. Pan X, Pike A, Joshi D, Bian G, McFadden MJ, Lu P, et al. The bacterium Wolbachia exploits host innate immunity to establish a symbiotic relationship with the dengue vector mosquito Aedes aegypti. ISME J. 2018;12: 277–288. doi:10.1038/ismej.2017.174

64. Christophides GK, Vlachou D, Kafatos FC. Comparative and functional genomics of the innate immune system in the malaria vector Anopheles gambiae. Immunol Rev. 2004;198: 127–148. doi:10.1111/j.0105-2896.2004.0127.x

65. Xi Z, Ramirez JL, Dimopoulos G. The Aedes aegypti Toll Pathway Controls Dengue Virus Infection. PLoS Pathog. 2008;4: e1000098. doi:10.1371/journal.ppat.1000098

66. Iatsenko I, Marra A, Boquete J-P, Peña J, Lemaitre B. Iron sequestration by transferrin 1 mediates nutritional immunity in Drosophila melanogaster. Proc Natl Acad Sci U S A. 2020;117: 7317–7325. doi:10.1073/pnas.1914830117

67. Mao W, Zeng Q, She L, Yuan H, Luo Y, Wang R, et al. Wolbachia Utilizes lncRNAs to Activate the Anti-Dengue Toll Pathway and Balance Reactive Oxygen Species Stress in Aedes aegypti Through a Competitive Endogenous RNA Network. Front Cell Infect Microbiol. 2022;11. Available: https://www.frontiersin.org/articles/10.3389/fcimb.2021.823403

68. Pan X, Zhou G, Wu J, Bian G, Lu P, Raikhel AS, et al. Wolbachia induces reactive oxygen species (ROS)-dependent activation of the Toll pathway to control dengue virus in the mosquito Aedes aegypti. Proc Natl Acad Sci U S A. 2012;109: E23–E31. doi:10.1073/pnas.1116932108

69. Ramirez JL, Muturi EJ, Barletta ABF, Rooney AP. The Aedes aegypti IMD pathway is a critical component of the mosquito antifungal immune response. Dev Comp Immunol. 2019;95: 1–9. doi:10.1016/j.dci.2018.12.010

70. Jiang H, Kanost MR. The clip-domain family of serine proteinases in arthropods. Insect Biochem Mol Biol. 2000;30: 95–105. doi:10.1016/S0965-1748(99)00113-7

71. Kanost MR, Jiang H. Clip-domain serine proteases as immune factors in insect hemolymph. Curr Opin Insect Sci. 2015;11: 47–55. doi:10.1016/j.cois.2015.09.003

72. Ji Y, Lu T, Zou Z, Wang Y. Aedes aegypti CLIPB9 activates prophenoloxidase-3 in the presence of CLIPA14 after fungal infection. Front Immunol. 2022;13: 927322. doi:10.3389/fimmu.2022.927322

73. Wang H-C, Wang Q-H, Bhowmick B, Li Y-X, Han Q. Functional characterization of two clip domain serine proteases in innate immune responses of Aedes aegypti. Parasit Vectors. 2021;14: 584. doi:10.1186/s13071-021-05091-9

74. Zou Z, Shin SW, Alvarez KS, Kokoza V, Raikhel AS. Distinct Melanization Pathways in the Mosquito Aedes aegypti. Immunity. 2010;32: 41–53. doi:10.1016/j.immuni.2009.11.011

75. Thomas P, Kenny N, Eyles D, Moreira LA, O'Neill SL, Asgari S. Infection with the wMel and wMelPop strains of Wolbachia leads to higher levels of melanization in the hemolymph of Drosophila melanogaster, Drosophila simulans and Aedes aegypti. Dev Comp Immunol. 2011;35: 360–365. doi:10.1016/j.dci.2010.11.007

76. Ye YH, Woolfit M, Rancès E, O'Neill SL, McGraw EA. Wolbachia-Associated Bacterial Protection in the Mosquito Aedes aegypti. PLoS Negl Trop Dis. 2013;7: e2362. doi:10.1371/journal.pntd.0002362

77. Etebari K, Hegde S, Saldaña MA, Widen SG, Wood TG, Asgari S, et al. Global Transcriptome Analysis of Aedes aegypti Mosquitoes in Response to Zika Virus Infection. mSphere. 2017;2: e00456-17. doi:10.1128/mSphere.00456-17

78. Maia RM, Valente V, Cunha MA, Sousa JF, Araujo DD, Silva WA, et al. Identification of unannotated exons of low abundance transcripts in Drosophila melanogaster and cloning of a new serine protease

gene upregulated upon injury. BMC Genomics. 2007;8: 249. doi:10.1186/1471-2164-8-249

79. Jones P, Binns D, Chang H-Y, Fraser M, Li W, McAnulla C, et al. InterProScan 5: genome-scale protein function classification. Bioinformatics. 2014;30: 1236–1240. doi:10.1093/bioinformatics/btu031

80. Pang X, Xiao X, Liu Y, Zhang R, Liu J, Liu Q, et al. Mosquito C-type lectins maintain gut microbiome homeostasis. Nat Microbiol. 2016;1: 16023. doi:10.1038/nmicrobiol.2016.23

81. Xia X, You M, Rao X-J, Yu X-Q. Insect C-type lectins in innate immunity. Dev Comp Immunol. 2018;83: 70–79. doi:10.1016/j.dci.2017.11.020

82. Adelman ZN, Myles KM. The C-Type Lectin Domain Gene Family in Aedes aegypti and Their Role in Arbovirus Infection. Viruses. 2018;10: 367. doi:10.3390/v10070367

83. Liu K, Qian Y, Jung Y-S, Zhou B, Cao R, Shen T, et al. mosGCTL-7, a C-Type Lectin Protein, Mediates Japanese Encephalitis Virus Infection in Mosquitoes. J Virol. 2017;91: e01348-16. doi:10.1128/JVI.01348-16

84. Williams M, Summers BJ, Baxter RHG. Biophysical Analysis of Anopheles gambiae Leucine-Rich Repeat Proteins APL1A1, APL1B and APL1C and Their Interaction with LRIM1. PLoS ONE. 2015;10: e0118911. doi:10.1371/journal.pone.0118911

85. Zhao L, Alto BW, Shin D. Transcriptional Profile of Aedes aegypti Leucine-Rich Repeat Proteins in Response to Zika and Chikungunya Viruses. Int J Mol Sci. 2019;20: 615. doi:10.3390/ijms20030615

86. Osta MA, Christophides GK, Kafatos FC. Effects of mosquito genes on Plasmodium development. Science. 2004;303: 2030–2032. doi:10.1126/science.1091789

87. Povelones M, Waterhouse RM, Kafatos FC, Christophides GK. Leucine-rich repeat protein complex activates mosquito complement in defense against Plasmodium parasites. Science. 2009;324: 258–261. doi:10.1126/science.1171400

88. Moita LF, Wang-Sattler R, Michel K, Zimmermann T, Blandin S, Levashina EA, et al. In Vivo Identification of Novel Regulators and Conserved Pathways of Phagocytosis in A. gambiae. Immunity. 2005;23: 65–73. doi:10.1016/j.immuni.2005.05.006

89. Burtenshaw SM, Su PP, Zhang JR, Tobe SS, Dayton L, Bendena WG. A putative farnesoic acid O-methyltransferase (FAMeT) orthologue in Drosophila melanogaster (CG10527): Relationship to juvenile hormone biosynthesis? Peptides. 2008;29: 242–251. doi:10.1016/j.peptides.2007.10.030

90. Yagi KJ, Konz KG, Stay B, Tobe SS. Production and utilization of farnesoic acid in the juvenile hormone biosynthetic pathway by corpora allata of larval Diploptera punctata. Gen Comp Endocrinol. 1991;81: 284–294. doi:10.1016/0016-6480(91)90013-V

91. Noriega FG. Juvenile Hormone Biosynthesis in Insects: What Is New, What Do We Know, and What Questions Remain? Int Sch Res Not. 2014;2014: 967361. doi:10.1155/2014/967361

92. Zou Z, Saha TT, Roy S, Shin SW, Backman TWH, Girke T, et al. Juvenile hormone and its receptor, methoprene-tolerant, control the dynamics of mosquito gene expression. Proc Natl Acad Sci. 2013;110: E2173–E2181. doi:10.1073/pnas.1305293110

93. Van Ekert E, Heylen K, Rougé P, Powell CA, Shatters RG, Smagghe G, et al. Aedes aegypti juvenile hormone acid methyl transferase, the ultimate enzyme in the biosynthetic pathway of juvenile hormone III, exhibits substrate control. J Insect Physiol. 2014;64: 62–73. doi:10.1016/j.jinsphys.2014.03.001

94. Liu C, Wang J-L, Zheng Y, Xiong E-J, Li J-J, Yuan L-L, et al. Wolbachia-induced paternal defect in Drosophila is likely by interaction with the juvenile hormone pathway. Insect Biochem Mol Biol. 2014;49: 49–58. doi:10.1016/j.ibmb.2014.03.014

95. Nouzova M, Edwards MJ, Michalkova V, Ramirez CE, Ruiz M, Areiza M, et al. Epoxidation of juvenile hormone was a key innovation improving insect reproductive fitness. Proc Natl Acad Sci. 2021;118: e2109381118. doi:10.1073/pnas.2109381118

96. Ramos LFC, Martins M, Murillo JR, Domont GB, de Oliveira DMP, Nogueira FCS, et al. Interspecies Isobaric Labeling-Based Quantitative Proteomics Reveals Protein Changes in the Ovary of Aedes aegypti Coinfected With ZIKV and Wolbachia. Front Cell Infect Microbiol. 2022;12. Available: https://www.frontiersin.org/articles/10.3389/fcimb.2022.900608

97. Sehlmeyer S, Wang L, Langel D, Heckel DG, Mohagheghi H, Petschenka G, et al. Flavin-Dependent Monooxygenases as a Detoxification Mechanism in Insects: New Insights from the Arctiids (Lepidoptera). PLOS ONE. 2010;5: e10435. doi:10.1371/journal.pone.0010435

98. Torres Pazmiño DE, Winkler M, Glieder A, Fraaije MW. Monooxygenases as biocatalysts: Classification, mechanistic aspects and biotechnological applications. J Biotechnol. 2010;146: 9–24. doi:10.1016/j.jbiotec.2010.01.021

99. Bailleul G, Yang G, Nicoll CR, Mattevi A, Fraaije MW, Mascotti ML. Evolution of enzyme

functionality in the flavin-containing monooxygenases. Nat Commun. 2023;14: 1042. doi:10.1038/s41467-023-36756-x

100. Veeravalli S, Phillips IR, Freire RT, Varshavi D, Everett JR, Shephard EA. Flavin-Containing Monooxygenase 1 Catalyzes the Production of Taurine from Hypotaurine. Drug Metab Dispos. 2020;48: 378–385. doi:10.1124/dmd.119.089995

101. Kumar A, Shrinet J, Sunil S. Chikungunya virus infection in Aedes aegypti is modulated by L-cysteine, taurine, hypotaurine and glutathione metabolism. PLoS Negl Trop Dis. 2023;17: e0011280. doi:10.1371/journal.pntd.0011280

102. Mallott M, Hamm S, Troczka BJ, Randall E, Pym A, Grant C, et al. A flavin-dependent monooxgenase confers resistance to chlorantraniliprole in the diamondback moth, Plutella xylostella. Insect Biochem Mol Biol. 2019;115: 103247. doi:10.1016/j.ibmb.2019.103247

103. Tan CH, Wong PJ, LI MI, Yang H, Ng LC, O'Neill SL. wMel limits zika and chikungunya virus infection in a Singapore Wolbachia-introgressed A. aegypti strain, wMel-Sg. PLoS Negl Trop Dis. 2017;11: e0005496. doi:10.1371/journal.pntd.0005496

104. Tallon AK, Hill SR, Ignell R. Sex and age modulate antennal chemosensory-related genes linked to the onset of host seeking in the yellow-fever mosquito, Aedes aegypti. Sci Rep. 2019;9: 43. doi:10.1038/s41598-018-36550-6

105. Marcombe S, Poupardin R, Darriet F, Reynaud S, Bonnet J, Strode C, et al. Exploring the molecular basis of insecticide resistance in the dengue vector Aedes aegypti: a case study in Martinique Island (French West Indies). BMC Genomics. 2009;10: 494. doi:10.1186/1471-2164-10-494

106. Alfonso-Parra C, Ahmed-Braimah YH, Degner EC, Avila FW, Villarreal SM, Pleiss JA, et al. Mating-Induced Transcriptome Changes in the Reproductive Tract of Female Aedes aegypti. PLoS Negl Trop Dis. 2016;10: e0004451. doi:10.1371/journal.pntd.0004451

107. Caragata EP, Rezende FO, Simões TC, Moreira LA. Diet-Induced Nutritional Stress and Pathogen Interference in Wolbachia-Infected Aedes aegypti. PLoS Negl Trop Dis. 2016;10: e0005158. doi:10.1371/journal.pntd.0005158

108. Ramirez JL, Dimopoulos G. The Toll immune signaling pathway control conserved anti-dengue defenses across diverse A. aegypti strains and against multiple dengue virus serotypes. Dev Comp

Immunol. 2010;34: 625–629. doi:10.1016/j.dci.2010.01.006

109. Caragata EP, Rocha MN, Pereira TN, Mansur SB, Dutra HLC, Moreira LA. Pathogen blocking in Wolbachia-infected Aedes aegypti is not affected by Zika and dengue virus co-infection. PLoS Negl Trop Dis. 2019;13: e0007443. doi:10.1371/journal.pntd.0007443

110. Xiao G, Liu Z-H, Zhao M, Wang H-L, Zhou B. Transferrin 1 Functions in Iron Trafficking and Genetically Interacts with Ferritin in Drosophila melanogaster. Cell Rep. 2019;26: 748-758.e5. doi:10.1016/j.celrep.2018.12.053

111. Zhu Y, Tong L, Nie K, Wiwatanaratanabutr I, Sun P, Li Q, et al. Host serum iron modulates dengue virus acquisition by mosquitoes. Nat Microbiol. 2019;4: 2405–2415. doi:10.1038/s41564-019-0555-x

112. Laurentino SS, Correia S, Cavaco JE, Oliveira PF, Sousa M de, Barros A, et al. Regucalcin, a calcium-binding protein with a role in male reproduction? Mol Hum Reprod. 2012;18: 161–170. doi:10.1093/molehr/gar075

113. Yamaguchi M. Role of Regucalcin in Maintaining Cell Homeostasis and Function (Review). Int J Mol Med. 2005;15: 371–89. doi:10.3892/ijmm.15.3.371

114. Syed ZA, Härd T, Uv A, Dijk-Härd IF van. A Potential Role for Drosophila Mucins in Development and Physiology. PLOS ONE. 2008;3: e3041. doi:10.1371/journal.pone.0003041

115. Finn RD, Bateman A, Clements J, Coggill P, Eberhardt RY, Eddy SR, et al. Pfam: the protein families database. Nucleic Acids Res. 2014;42: D222–D230. doi:10.1093/nar/gkt1223

116. Adams MD, Celniker SE, Holt RA, Evans CA, Gocayne JD, Amanatides PG, et al. The Genome Sequence of Drosophila melanogaster. Science. 2000;287: 2185–2195. doi:10.1126/science.287.5461.2185

117. Miller WJ, Ehrman L, Schneider D. Infectious Speciation Revisited: Impact of Symbiont-Depletion on Female Fitness and Mating Behavior of Drosophila paulistorum. PLOS Pathog. 2010;6: e1001214. doi:10.1371/journal.ppat.1001214

118. Zug R, Hammerstein P. Bad guys turned nice? A critical assessment of Wolbachia mutualisms in arthropod hosts. Biol Rev. 2015;90: 89–111. doi:10.1111/brv.12098

119. Bian G, Zhou G, Lu P, Xi Z. Replacing a native Wolbachia with a novel strain results in an increase in endosymbiont load and resistance to dengue virus in a mosquito vector. PLoS Negl Trop Dis. 2013;7:

e2250. doi:10.1371/journal.pntd.0002250

120. Wong ZS, Brownlie JC, Johnson KN. Oxidative Stress Correlates with Wolbachia-Mediated Antiviral Protection in Wolbachia-Drosophila Associations. Appl Environ Microbiol. 2015;81: 3001–3005. doi:10.1128/AEM.03847-14

121. He L, He T, Farrar S, Ji L, Liu T, Ma X. Antioxidants Maintain Cellular Redox Homeostasis by Elimination of Reactive Oxygen Species. Cell Physiol Biochem Int J Exp Cell Physiol Biochem Pharmacol. 2017;44: 532–553. doi:10.1159/000485089

122. Cho K-O, Kim G-W, Lee O-K. Wolbachia bacteria reside in host Golgi-related vesicles whose position is regulated by polarity proteins. PloS One. 2011;6: e22703. doi:10.1371/journal.pone.0022703

123. Fattouh N, Cazevieille C, Landmann F. Wolbachia endosymbionts subvert the endoplasmic reticulum to acquire host membranes without triggering ER stress. PLoS Negl Trop Dis. 2019;13: e0007218. doi:10.1371/journal.pntd.0007218

124. Berridge MJ, Lipp P, Bootman MD. The versatility and universality of calcium signalling. Nat Rev Mol Cell Biol. 2000;1: 11–21. doi:10.1038/35036035

125. Cohen E. Chitin synthesis and degradation as targets for pesticide action. Arch Insect Biochem Physiol. 1993;22: 245–261. doi:10.1002/arch.940220118

126. Farnesi LC, Menna-Barreto RFS, Martins AJ, Valle D, Rezende GL. Physical features and chitin content of eggs from the mosquito vectors Aedes aegypti, Anopheles aquasalis and Culex quinquefasciatus: Connection with distinct levels of resistance to desiccation. J Insect Physiol. 2015;83: 43–52. doi:10.1016/j.jinsphys.2015.10.006

127. Sigle LT, McGraw EA. Expanding the canon: Non-classical mosquito genes at the interface of arboviral infection. Insect Biochem Mol Biol. 2019;109: 72–80. doi:10.1016/j.ibmb.2019.04.004

128. Udaya Prakash NA, Jayanthi M, Sabarinathan R, Kangueane P, Mathew L, Sekar K. Evolution, Homology Conservation, and Identification of Unique Sequence Signatures in GH19 Family Chitinases. J Mol Evol. 2010;70: 466–478. doi:10.1007/s00239-010-9345-z

129. Zhang X, Zhang J, Park Y, Zhu KY. Identification and characterization of two chitin synthase genes in African malaria mosquito, Anopheles gambiae. Insect Biochem Mol Biol. 2012;42: 674–682. doi:10.1016/j.ibmb.2012.05.005

130. Geoghegan V, Stainton K, Rainey SM, Ant TH, Dowle AA, Larson T, et al. Perturbed cholesterol and vesicular trafficking associated with dengue blocking in Wolbachia-infected Aedes aegypti cells. Nat Commun. 2017;8: 526. doi:10.1038/s41467-017-00610-8

131. Quek S, Cook DAN, Wu Y, Marriott AE, Steven A, Johnston KL, et al. Wolbachia depletion blocks transmission of lymphatic filariasis by preventing chitinase-dependent parasite exsheathment. Proc Natl Acad Sci U S A. 2022;119: e2120003119. doi:10.1073/pnas.2120003119

132. Allman MJ, Fraser JE, Ritchie SA, Joubert DA, Simmons CP, Flores HA. Wolbachia's Deleterious Impact on Aedes aegypti Egg Development: The Potential Role of Nutritional Parasitism. Insects. 2020;11: 735. doi:10.3390/insects11110735

133. Rezende GL, Martins AJ, Gentile C, Farnesi LC, Pelajo-Machado M, Peixoto AA, et al. Embryonic desiccation resistance in Aedes aegypti: presumptive role of the chitinized Serosal Cuticle. BMC Dev Biol. 2008;8: 82. doi:10.1186/1471-213X-8-82

134. Farnesi LC, Belinato TA, Gesto JSM, Martins AJ, Bruno RV, Moreira LA. Embryonic development and egg viability of wMel-infected Aedes aegypti. Parasit Vectors. 2019;12: 211. doi:10.1186/s13071-019-3474-z

135. Henrichfreise B, Schiefer A, Schneider T, Nzukou E, Poellinger C, Hoffmann T-J, et al. Functional conservation of the lipid II biosynthesis pathway in the cell wall-less bacteria Chlamydia and Wolbachia: why is lipid II needed? Mol Microbiol. 2009;73: 913–923. doi:10.1111/j.1365-2958.2009.06815.x

136. Vollmer J, Schiefer A, Schneider T, Jülicher K, Johnston KL, Taylor MJ, et al. Requirement of lipid II biosynthesis for cell division in cell wall-less Wolbachia, endobacteria of arthropods and filarial nematodes. Int J Med Microbiol. 2013;303: 140–149. doi:10.1016/j.ijmm.2013.01.002

137. Kanehisa M, Furumichi M, Sato Y, Kawashima M, Ishiguro-Watanabe M. KEGG for taxonomy-based analysis of pathways and genomes. Nucleic Acids Res. 2023;51: D587–D592. doi:10.1093/nar/gkac963

138. Sacoman JL, Hollingsworth RI. Synthesis and evaluation of an N-acetylglucosamine biosynthesis inhibitor. Carbohydr Res. 2011;346: 2294–2299. doi:10.1016/j.carres.2011.07.004

139. Wilmes M, Meier K, Schiefer A, Josten M, Otten CF, Klöckner A, et al. AmiD Is a Novel Peptidoglycan Amidase in Wolbachia Endosymbionts of Drosophila melanogaster. Front Cell Infect Microbiol. 2017;7:

353. doi:10.3389/fcimb.2017.00353

140. Caragata EP, Rancès E, O'Neill SL, McGraw EA. Competition for amino acids between Wolbachia and the mosquito host, Aedes aegypti. Microb Ecol. 2014;67: 205–218. doi:10.1007/s00248-013-0339-4

141. Jiménez NE, Gerdtzen ZP, Olivera-Nappa Á, Salgado JC, Conca C. A systems biology approach for studying Wolbachia metabolism reveals points of interaction with its host in the context of arboviral infection. PLoS Negl Trop Dis. 2019;13: e0007678. doi:10.1371/journal.pntd.0007678

142. Jiménez NE, Gerdtzen ZP, Olivera-Nappa Á, Salgado JC, Conca C. Novel Symbiotic Genome-Scale Model Reveals Wolbachia's Arboviral Pathogen Blocking Mechanism in Aedes aegypti. mBio. 2021;12: e01563-21. doi:10.1128/mBio.01563-21

143. White PM, Serbus LR, Debec A, Codina A, Bray W, Guichet A, et al. Reliance of Wolbachia on High Rates of Host Proteolysis Revealed by a Genome-Wide RNAi Screen of Drosophila Cells. Genetics. 2017;205: 1473–1488. doi:10.1534/genetics.116.198903

144. Dale C, Welburn SC. The endosymbionts of tsetse flies: manipulating host-parasite interactions. Int J Parasitol. 2001;31: 628–631. doi:10.1016/s0020-7519(01)00151-5

145. Dias RO, Cardoso C, Pimentel AC, Damasceno TF, Ferreira C, Terra WR. The roles of mucus-forming mucins, peritrophins and peritrophins with mucin domains in the insect midgut. Insect Mol Biol. 2018;27: 46–60. doi:10.1111/imb.12340

Supporting information

S1 Table. Datasets included and excluded from this study.

S2 Table. RNA-Seq mapping statistics. Number of reads in each RNA-Seq dataset and percentage of reads mapped to the *A. aegypti* reference genome.

S1 Fig. Microarray MA-plots. MA-plots of two-channel microarray data from Kambris et al. (2009) (left), Rancès et al. (2012) (middle) and Ye et al. (2013) (right). MA-plots show M values (logarithmic fold-change between red and green intensities for each spot) versus A values (average of logarithmic red and green intensities for each spot). Control spots are colored (gray = dark control, purple = bright control, red = 10-fold

upregulated, orange = 3-fold upregulated, pink = 3-fold downregulated, blue = 10-fold downregulated, yellow = non-differentially expressed.

S3 Table. Gene set enrichment analysis results. GSEA results for each gene list derived from a comparison between an infected and an uninfected condition. GSEA leading edges are filtered to include only differentially expressed genes ($p<0.05$).

S4 Table. Meta-analysis results. Results from meta-analysis of *p*-values derived from GSEA and differential expression analyses.

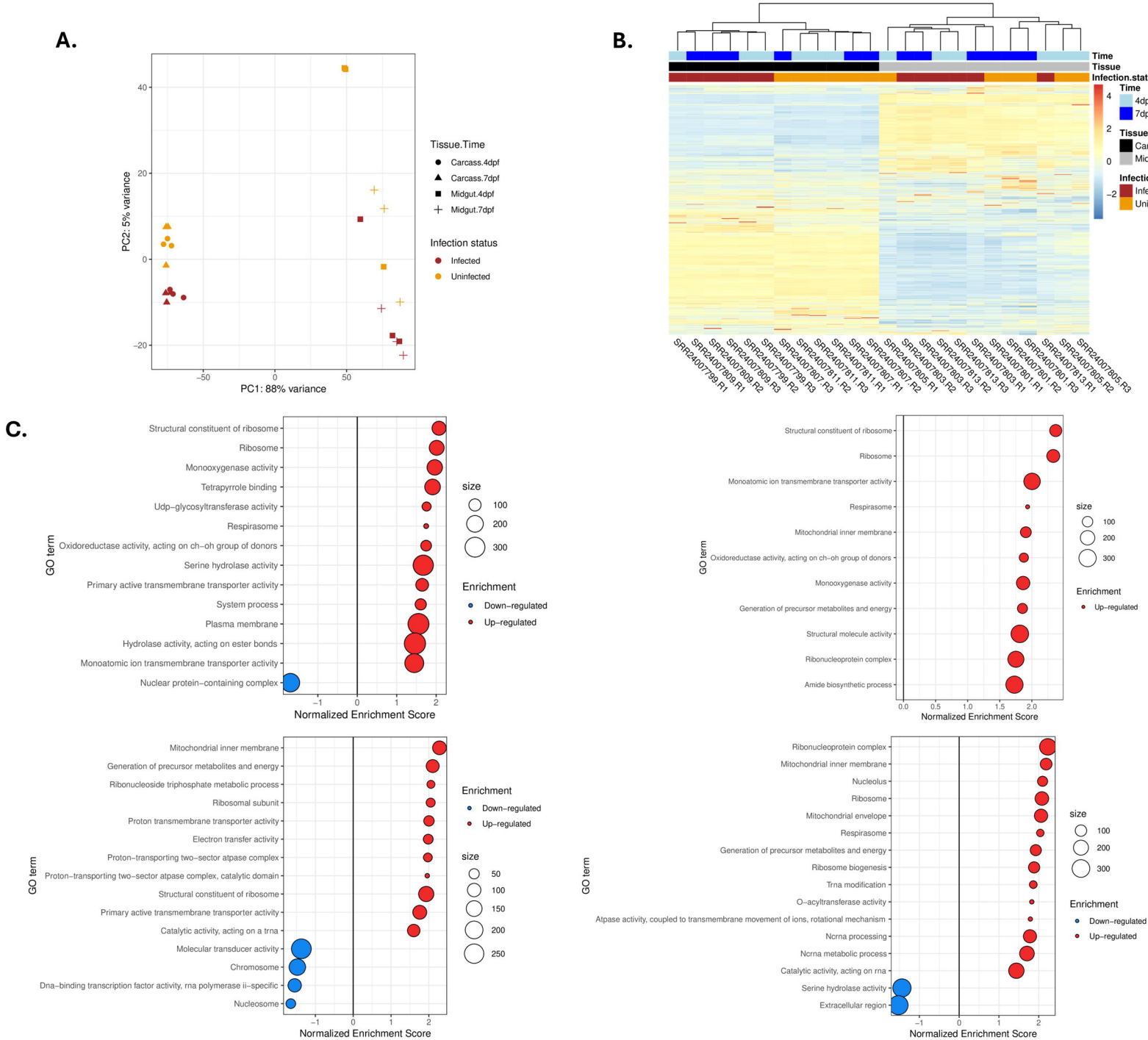
A.
PC2: 5% variance
PC1: 88% variance
Tissue.Time
Carcass.4dpf
Carcass.7dpf
Midgut.4dpf
Midgut.7dpf
Infection status
Infected
Uninfected
B.
Time
Tissue
Infection.status
4dpf
7dpf
Carcass
Midgut
Infected
Uninfected
C.
GO term
Normalized Enrichment Score
size
Enrichment
Down−regulated
Up−regulated
Structural constituent of ribosome
Ribosome
Monooxygenase activity
Tetrapyrrole binding
Udp−glycosyltransferase activity
Respirasome
Oxidoreductase activity, acting on ch−oh group of donors
Serine hydrolase activity
Primary active transmembrane transporter activity
System process
Plasma membrane
Hydrolase activity, acting on ester bonds
Monoatomic ion transmembrane transporter activity
Nuclear protein−containing complex
Mitochondrial inner membrane
Generation of precursor metabolites and energy
Ribonucleoside triphosphate metabolic process
Ribosomal subunit
Proton transmembrane transporter activity
Electron transfer activity
Proton−transporting two−sector atpase complex
Proton−transporting two−sector atpase complex, catalytic domain
Catalytic activity, acting on a trna
Molecular transducer activity
Chromosome
Dna−binding transcription factor activity, rna polymerase ii−specific
Nucleosome
Monoatomic ion transmembrane transporter activity
Structural molecule activity
Ribonucleoprotein complex
Amide biosynthetic process
Nucleolus
Mitochondrial envelope
Ribosome biogenesis
Trna modification
O−acyltransferase activity
Atpase activity, coupled to transmembrane movement of ions, rotational mechanism
Ncrna processing
Ncrna metabolic process
Extracellular region

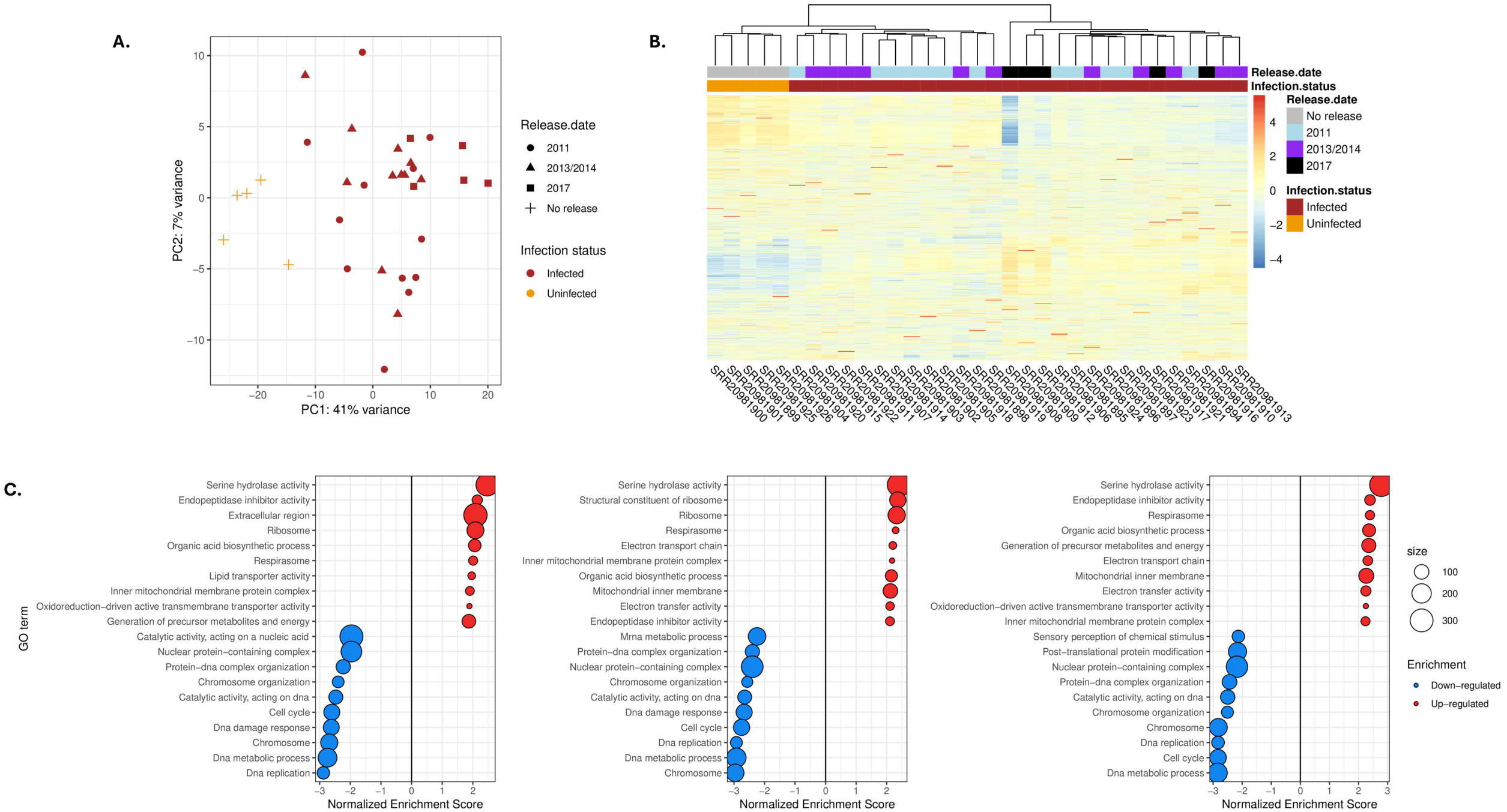
A.
PC2: 7% variance
PC1: 41% variance
Release.date
2011
2013/2014
2017
No release
Infection status
Infected
Uninfected
B.
Release.date
Infection.status
No release
2011
2013/2014
2017
Infected
Uninfected
C.
GO term
Serine hydrolase activity
Endopeptidase inhibitor activity
Extracellular region
Ribosome
Organic acid biosynthetic process
Respirasome
Lipid transporter activity
Inner mitochondrial membrane protein complex
Oxidoreduction−driven active transmembrane transporter activity
Generation of precursor metabolites and energy
Catalytic activity, acting on a nucleic acid
Nuclear protein−containing complex
Protein−dna complex organization
Chromosome organization
Catalytic activity, acting on dna
Cell cycle
Dna damage response
Chromosome
Dna metabolic process
Dna replication
Structural constituent of ribosome
Electron transport chain
Mitochondrial inner membrane
Mrna metabolic process
Electron transfer activity
Sensory perception of chemical stimulus
Post−translational protein modification
Normalized Enrichment Score
size
Enrichment
Down−regulated
Up−regulated

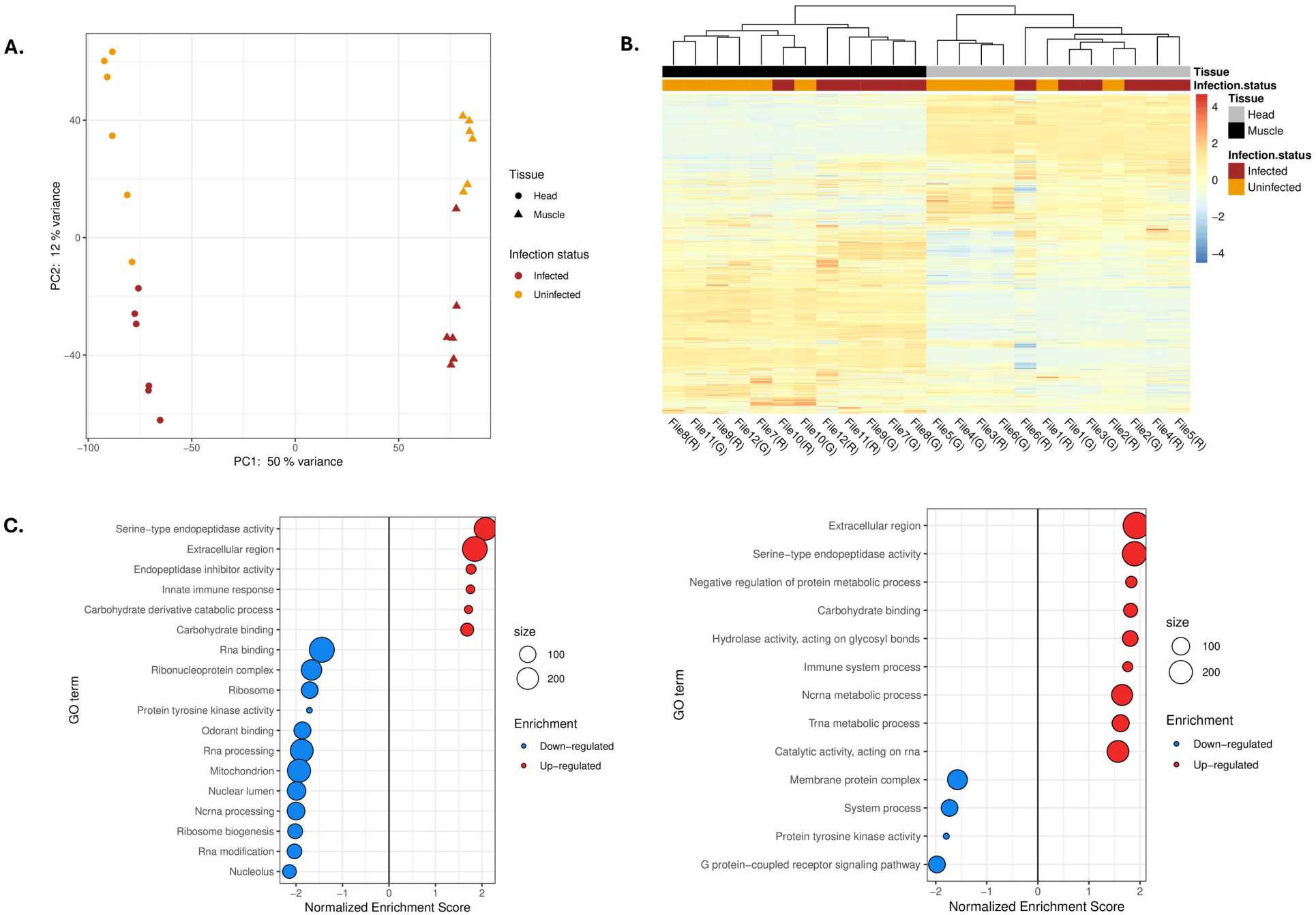
A.
PC2: 12 % variance
PC1: 50 % variance
Tissue
Head
Muscle
Infection status
Infected
Uninfected
B.
Tissue
Infection.status
Head
Muscle
Infected
Uninfected
File8(R)
File11(G)
File9(R)
File12(G)
File7(R)
File10(R)
File10(G)
File12(R)
File11(R)
File9(G)
File7(G)
File8(G)
File5(G)
File4(G)
File3(R)
File6(G)
File6(R)
File1(R)
File1(G)
File3(G)
File2(R)
File2(G)
File4(R)
File5(R)
C.
GO term
Serine−type endopeptidase activity
Extracellular region
Endopeptidase inhibitor activity
Innate immune response
Carbohydrate derivative catabolic process
Carbohydrate binding
Rna binding
Ribonucleoprotein complex
Ribosome
Protein tyrosine kinase activity
Odorant binding
Rna processing
Mitochondrion
Nuclear lumen
Ncrna processing
Ribosome biogenesis
Rna modification
Nucleolus
Normalized Enrichment Score
size
Enrichment
Down−regulated
Up−regulated
Extracellular region
Serine−type endopeptidase activity
Negative regulation of protein metabolic process
Carbohydrate binding
Hydrolase activity, acting on glycosyl bonds
Immune system process
Ncrna metabolic process
Trna metabolic process
Catalytic activity, acting on rna
Membrane protein complex
System process
Protein tyrosine kinase activity
G protein−coupled receptor signaling pathway

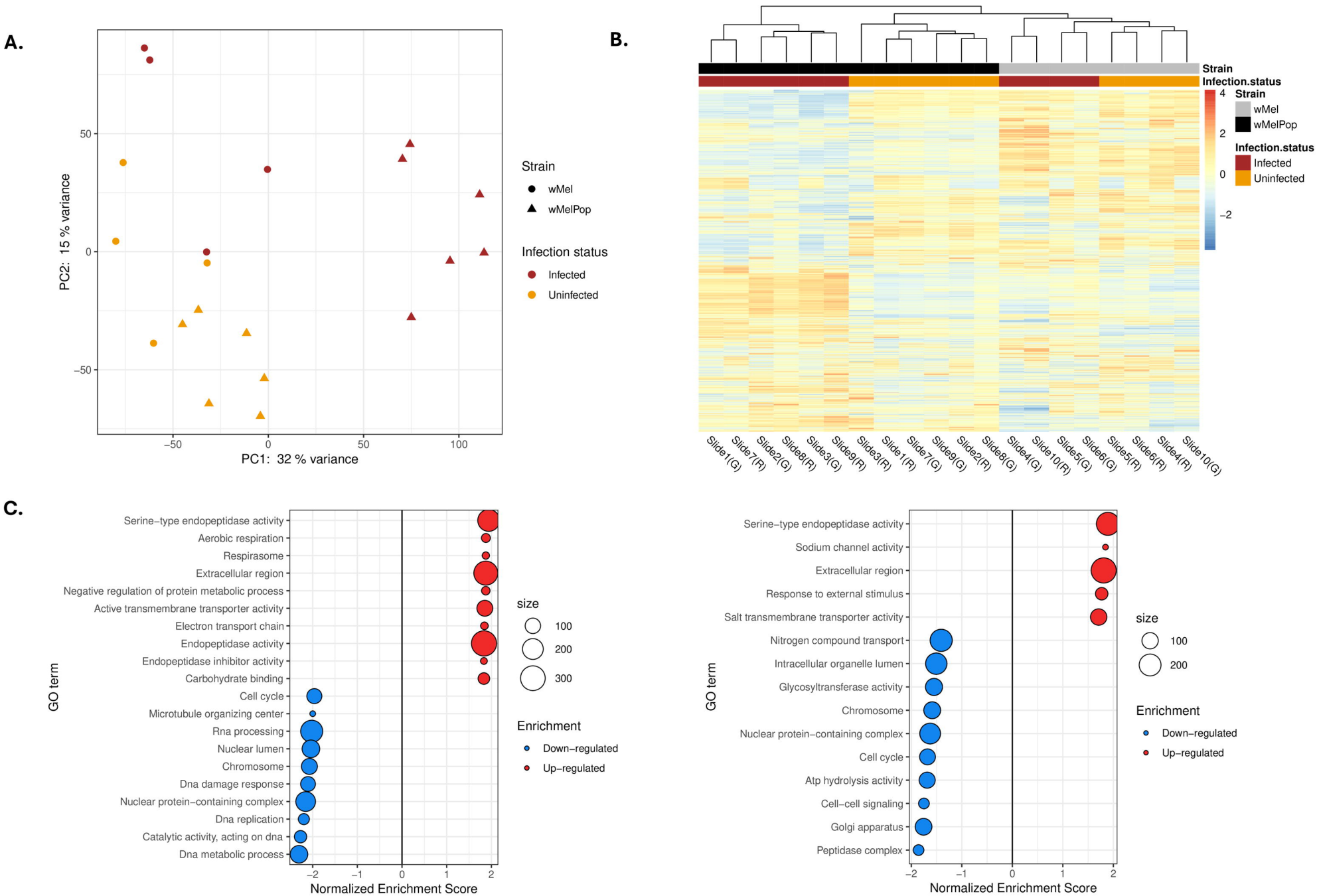
A.
PC2: 15 % variance
PC1: 32 % variance
Strain
wMel
wMelPop
Infection status
Infected
Uninfected
B.
Strain
Infection.status
Slide1(G)
Slide7(R)
Slide2(G)
Slide8(R)
Slide3(G)
Slide9(R)
Slide3(R)
Slide1(R)
Slide7(G)
Slide9(G)
Slide2(R)
Slide8(G)
Slide4(G)
Slide10(R)
Slide5(G)
Slide6(G)
Slide5(R)
Slide6(R)
Slide4(R)
Slide10(G)
C.
GO term
Serine−type endopeptidase activity
Aerobic respiration
Respirasome
Extracellular region
Negative regulation of protein metabolic process
Active transmembrane transporter activity
Electron transport chain
Endopeptidase activity
Endopeptidase inhibitor activity
Carbohydrate binding
Cell cycle
Microtubule organizing center
Rna processing
Nuclear lumen
Chromosome
Dna damage response
Nuclear protein−containing complex
Dna replication
Catalytic activity, acting on dna
Dna metabolic process
Normalized Enrichment Score
size
Enrichment
Down−regulated
Up−regulated
Serine−type endopeptidase activity
Sodium channel activity
Extracellular region
Response to external stimulus
Salt transmembrane transporter activity
Nitrogen compound transport
Intracellular organelle lumen
Glycosyltransferase activity
Chromosome
Nuclear protein−containing complex
Cell cycle
Atp hydrolysis activity
Cell−cell signaling
Golgi apparatus
Peptidase complex
Normalized Enrichment Score
size
Enrichment
Down−regulated
Up−regulated

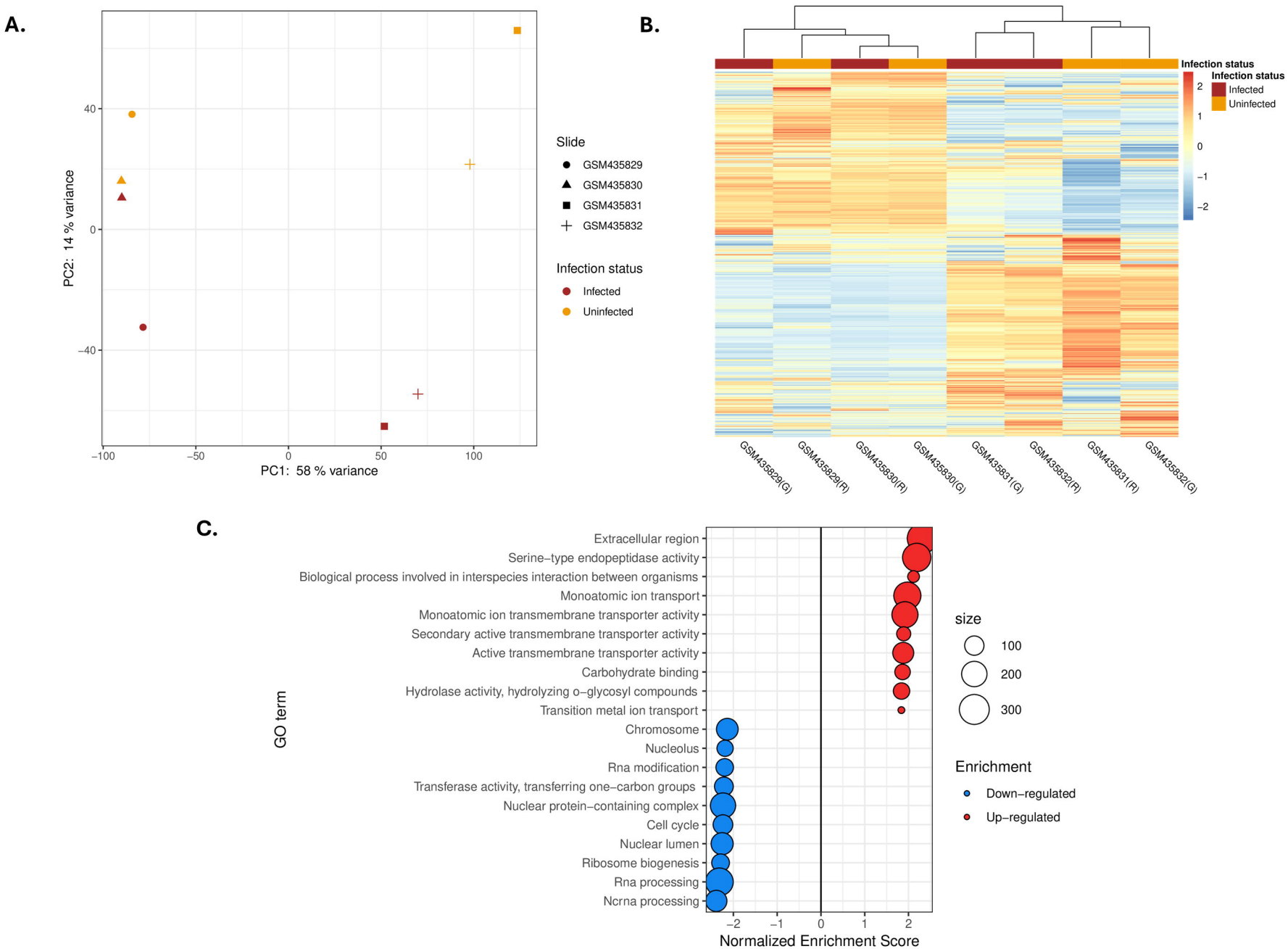
A.
PC2: 14 % variance
PC1: 58 % variance
40
0
−40
−100
−50
0
50
100
Slide
GSM435829
GSM435830
GSM435831
GSM435832
Infection status
Infected
Uninfected
B.
Infection status
Infected
Uninfected
2
1
0
−1
−2
GSM435829(G)
GSM435829(R)
GSM435830(R)
GSM435830(G)
GSM435831(G)
GSM435832(R)
GSM435831(R)
GSM435832(G)
C.
GO term
Extracellular region
Serine−type endopeptidase activity
Biological process involved in interspecies interaction between organisms
Monoatomic ion transport
Monoatomic ion transmembrane transporter activity
Secondary active transmembrane transporter activity
Active transmembrane transporter activity
Carbohydrate binding
Hydrolase activity, hydrolyzing o−glycosyl compounds
Transition metal ion transport
Chromosome
Nucleolus
Rna modification
Transferase activity, transferring one−carbon groups
Nuclear protein−containing complex
Cell cycle
Nuclear lumen
Ribosome biogenesis
Rna processing
Ncrna processing
−2
−1
0
1
2
Normalized Enrichment Score
size
100
200
300
Enrichment
Down−regulated
Up−regulated